Note: This copy is for your personal non-commercial use only. To order presentation-ready copies for distribution to your colleagues or clients, contact us at *www.rsna.org/rsnarights.*

Multidetector CT of Vascular Compression Syndromes in the Abdomen and Pelvis[1]

Ramit Lamba, MBBS, MD
Dawn T. Tanner, MD
Simran Sekhon, MBBS
John P. McGahan, MD
Michael T. Corwin, MD
Chandana G. Lall, MD

Abbreviations: AMA = aortomesenteric angle, AMD = aortomesenteric distance, CIA = common iliac artery, CIV = common iliac vein, IVC = inferior vena cava, IVU = intravenous urography, LRV = left renal vein, MALS = median arcuate ligament syndrome, MIP = maximum intensity projection, MPR = multiplanar reformation, OVS = ovarian vein syndrome, SMA = superior mesenteric artery, 3D = three-dimensional, UPJ = ureteropelvic junction, VR = volume-rendered

RadioGraphics 2014; 34:93–115

Published online 10.1148/rg.341125010

Content Codes: CT GI IR VA

[1]From the Department of Radiology, University of California, Davis Health System, 4860 Y St, Suite 3100, Sacramento, CA 95817 (R.L., D.T.T., S.S., J.P.M., M.T.C.); and Department of Radiology, University of California, Irvine Medical Center, Irvine, Calif (C.G.L). Presented as an education exhibit at the 2010 RSNA Annual Meeting. Received February 3, 2012; revision requested April 20; final revision received April 11, 2013; accepted April 25. For this journal-based SA-CME activity, the authors, editor, and reviewers have no financial relationships to disclose. **Address correspondence to** R.L. (e-mail: *ramit.lamba@ucdmc.ucdavis.edu*).

SA-CME LEARNING OBJECTIVES FOR TEST 3

After completing this journal-based SA-CME activity, participants will be able to:

- Describe the compression of hollow visceral structures and blood vessels caused by surrounding abdominopelvic structures.
- List the clinical signs and symptoms of the various abdominal and pelvic compression syndromes.
- Discuss the key imaging features of these syndromes at different modalities.

See www.rsna.org/education/search/RG

TEACHING POINTS

See last page

Certain abdominopelvic vascular structures may be compressed by adjacent anatomic structures or may cause compression of adjacent hollow viscera. Such compressions may be asymptomatic; when symptomatic, however, they can lead to a variety of uncommon syndromes in the abdomen and pelvis, including median arcuate ligament syndrome, May-Thurner syndrome, nutcracker syndrome, superior mesenteric artery syndrome, ureteropelvic junction obstruction, ovarian vein syndrome, and other forms of ureteral compression. These syndromes, the pathogenesis of some of which remains controversial, can result in nonspecific symptoms of epigastric or flank pain, weight loss, nausea and vomiting, hematuria, or urinary tract infection. Direct venography or duplex ultrasonography can provide hemodynamic information in cases of vascular compression. However, multidetector computed tomography is particularly useful in that it allows a comprehensive single-study evaluation of the anatomy and resultant morphologic changes. Anatomic findings that can predispose to these syndromes may be encountered in patients who are undergoing imaging for unrelated reasons. However, the diagnosis of these syndromes should not be made on the basis of imaging findings alone. Severely symptomatic patients require treatment, which is generally surgical, although endovascular techniques are increasingly being used to treat venous compressions.

©RSNA, 2014 • *radiographics.rsna.org*

Introduction

Vascular structures in the abdomen and pelvis may be compressed by adjacent anatomic structures, or they may cause compression of adjacent hollow viscera. Thus, compression of the proximal celiac artery, transverse duodenum, left common iliac vein (CIV), left renal vein (LRV), ureteropelvic junction (UPJ), and ureter can occur due to their close anatomic relationship to adjacent ligaments as well as bony and vascular structures. When symptomatic, such compressions can result in a variety of uncommon syndromes in the abdomen and pelvis, including median arcuate ligament syndrome (MALS), May-Thurner syndrome, nutcracker syndrome, superior mesenteric artery (SMA) syndrome, UPJ obstruction, ovarian vein syndrome (OVS), and other forms of ureteral compression (Table). In this article, we refer to this heterogeneous group of disorders as "vascular compression syndromes," since they all involve either the compression *of* vascular structures or the compression of hollow viscera *by* vascular structures.

Teaching Point

Controversy surrounds the pathogenesis of some of these syndromes. Anatomic or morphologic findings that predispose to such compression may occasionally be encountered in asymptomatic patients who undergo imaging for unrelated causes. Thus, caution should be exercised to avoid overdiagnosis of these syndromes. It is important that the diagnosis of these syndromes not be based on imaging findings alone.

Teaching Point

Vascular Compression Syndromes in the Abdomen and Pelvis

Syndrome	Compressed Structure	Cause of Compression	Primary Clinical Symptoms	Multidetector CT Findings	Treatment
MALS	Celiac artery	Median arcuate ligament	Epigastric pain, weight loss	Proximal celiac artery narrowing with a "hooked" appearance, celiac artery–SMA collateral vessels, possible formation of PDA aneurysms	Resection of ligament with or without vascular reconstruction or bypass surgery
May-Thurner syndrome	Left CIV	Right CIA and vertebral body	Left lower extremity swelling, deep venous thrombosis	Left CIV compression with or without left iliac and proximal femoral vein thrombosis	Thrombolysis and iliac vein stent placement
Nutcracker syndrome	LRV	SMA and aorta	Left flank pain, hematuria	LRV compression; left renal hilar, periureteral, and pelvic varices; dilated left gonadal vein; reduced AMA and AMD	Conservative management, renal vein transposition or bypass surgery, renal vein stent placement, gonadal vein embolization or bypass surgery
SMA syndrome	Transverse duodenum	SMA and aorta	Epigastric pain, weight loss, nausea/vomiting	Mid-transverse duodenal compression, dilated stomach and proximal duodenum, reduced AMA and AMD	Conservative management, bowel bypass surgery (duodenojejunostomy)
UPJ obstruction	UPJ	Crossing renal artery or vein, aperistaltic segment, or periureteral fibrosis	Flank pain, pyelonephritis, hematuria	Ballooned renal pelvis and hydronephrosis, with or without a crossing vessel at the UPJ	Pyeloplasty, endopyelotomy
OVS	Distal ureter	Crossing gonadal vein	Flank pain, hematuria	Hydronephrosis, hydroureter, crossing gonadal vessel at transition point	Embolization of ovarian vein
Retrocaval ureter	Proximal ureter	IVC and vertebral body	Flank pain, hematuria	Hydronephrosis and proximal hydroureter, "reverse J" configuration of proximal ureter with a retrocaval course	Ureteroureterostomy

Note.—AMA = aortomesenteric angle, AMD = aortomesenteric distance, CT = computed tomography, IVC = inferior vena cava, PDA = pancreaticoduodenal arcade.

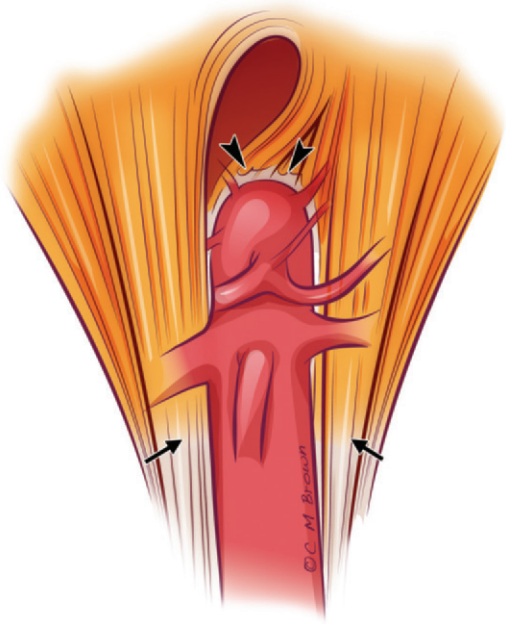

Figure 1. Drawing illustrates the anatomy of the median arcuate ligament (arrowheads), which connects the right and left crura of the diaphragm (arrows) at the level of the aortic hiatus, just superior to the origin of the celiac axis.

Symptoms resulting from such compressions can be vague, nonspecific, and obscure, resulting in delayed, incorrect, or missed diagnoses. Although many of these syndromes were described decades ago, they remain poorly understood. If unrecognized and untreated, they can be associated with significant morbidity. These syndromes may be encountered by physicians in a variety of disciplines and can present a diagnostic dilemma. For all of these reasons, it is important that these syndromes be recognized.

Multidetector computed tomography (CT) is the imaging modality of choice for many of these syndromes owing to its high contrast and high spatial and temporal resolution, capacity for obtaining isotropic data sets that allow multiplanar two-dimensional and three-dimensional (3D) postprocessing, remarkable accuracy, widespread accessibility, speed, and relative noninvasiveness. CT is best performed on multidetector CT scanners with 16 or more detector rows. Multiplanar reformation (MPR) can be performed, not just in sagittal and coronal planes, but in any defined anatomic plane, thereby providing a novel perspective that is customized to the unique anatomy of the patient. By incorporating MPR and 3D volume rendering (VR), multidetector CT is truly 3D. Maximum intensity projection (MIP) techniques greatly enhance the depiction of vascular structures at CT angiography. However, radiation exposure to younger patients, especially premenopausal women, needs to be considered. Ultrasonography (US) is largely operator, patient, and region dependent, although duplex US can provide information on the hemodynamic significance of vascular compressions. Most non–cross-sectional imaging techniques have limitations in the evaluation of these syndromes, but direct venography remains valuable in the diagnosis of syndromes that involve venous compression. In this article, we aim to familiarize radiologists with the multidetector CT appearance of these syndromes and the added benefit of MPR in diagnosis.

When conservative management is not indicated or fails, surgery is the mainstay for treatment. Open surgical techniques are now being replaced by less invasive laparoscopic techniques. Outcomes following surgery may vary, and the decision to treat should be made only in those patients who are experiencing disabling or severe symptoms.

In this article, we review vascular compression syndromes in the abdomen and pelvis in terms of relevant anatomy, pathogenesis, clinical presentations, imaging findings (with emphasis on findings at multidetector CT), and treatment options.

Median Arcuate Ligament Syndrome

MALS, also known as celiac artery compression syndrome or Dunbar syndrome, was first described in 1963 by Harjola (1). It is rare and is considered to be present when narrowing of the proximal celiac trunk by the median arcuate ligament results in clinical symptoms of epigastric pain and weight loss.

Anatomy and Pathogenesis

The median arcuate ligament is an archlike fibrous band connecting the right and left diaphragmatic crura at the level of the aortic hiatus, crossing the aorta anteriorly just superior to the celiac artery at the level of the first lumbar vertebral body (Fig 1) (2).

Compression of the proximal celiac artery by the median arcuate ligament may result if the celiac artery has a more cephalad origin or if the ligament is abnormally low (3). Compression typically increases during expiration as the aorta and celiac artery move superiorly.

Because of the large increase in the number of abdominal CT examinations in the past decade, coupled with the ability to obtain sagittal reconstructed images at CT, proximal celiac compression is occasionally seen incidentally in patients who are undergoing CT for unrelated reasons (4). Very few studies have investigated the incidence of celiac artery narrowing in asymptomatic adult patients. An evaluation of CT

a. b.

Figure 2. MALS in a 28-year-old man with chronic upper abdominal pain, postprandial nausea, loss of appetite, and a weight loss of 20 pounds over a 2-year period. **(a)** Midline sagittal reformatted MIP image from an abdominal CT angiographic study in deep inspiration shows a mild indentation on the superior aspect of the proximal celiac artery (arrow). **(b)** Midline sagittal reformatted MIP image in deep expiration shows a marked increase in the proximal celiac stenosis (arrow). The median arcuate ligament "tents" the superior aspect of the proximal celiac artery, resulting in the characteristic hooked appearance. In addition, mild poststenotic celiac dilatation is seen. A prominent pancreaticoduodenal collateral vessel (not shown) was also present.

angiographic findings obtained at full inspiration in 155 healthy asymptomatic kidney donors between 18 and 65 years of age showed narrowing of the celiac artery origin by more than 50% in eight individuals (5.2%). No significant collateral vessels were seen in any of the donors (5). To our knowledge, there are no published studies of the prevalence of MALS in the general population. In any case, such a study would be especially difficult to perform given the controversy that surrounds the definition of MALS. In 97 patients without any symptoms of mesenteric ischemia who were undergoing upper abdominal magnetic resonance (MR) angiography, narrowing of the proximal celiac artery by over 60% was present in 16 patients (16.5%) at end expiration and in 12 patients (12.4%) at full inspiration, findings that confirmed that compression of the celiac artery is more common during expiration (6).

Teaching Point

Thus, isolated celiac compression during expiration may not be clinically significant. Severe compression occurs in only a small percentage of patients and may cause symptoms (4). The pathophysiology of MALS is poorly characterized, and a causal relationship between the celiac narrowing and symptoms has not been completely established. Some vascular surgeons believe that two of the three mesenteric arteries must be occluded or severely stenotic to produce symptoms of chronic mesenteric ischemia (7), although this view has been refuted by others (8). In MALS, the SMA and inferior mesenteric artery are usually widely patent. Additionally, in cases of severe compression, hemodynamic compensation can result from the development of collateral vessels between the SMA and celiac branches. Therefore, it is probable that symptoms of mesenteric ischemia in MALS result from a "steal syndrome," with blood flow diverted from the SMA to the celiac branches. Finally, surgical correction of the compression does not always relieve symptoms.

Clinical Presentation

Most patients with celiac compression have no symptoms (4,6,9). When present, symptoms are more commonly seen in younger women and typically consist of epigastric pain (which may or may not be postprandial) and weight loss. An abdominal bruit may sometimes be detected at physical examination. Diagnosis is challenging and is based on the presence of symptoms, typical imaging findings, and exclusion of other causes.

Radiologic Findings

Typical findings can be seen at conventional mesenteric, CT, or MR angiography. Focal narrowing of the proximal celiac artery is seen, a finding that can be more pronounced in end expiration (Fig 2). The narrowed segment has a characteristic hooked appearance (Figs 2, 3). This appearance, along with the absence of atherosclerotic

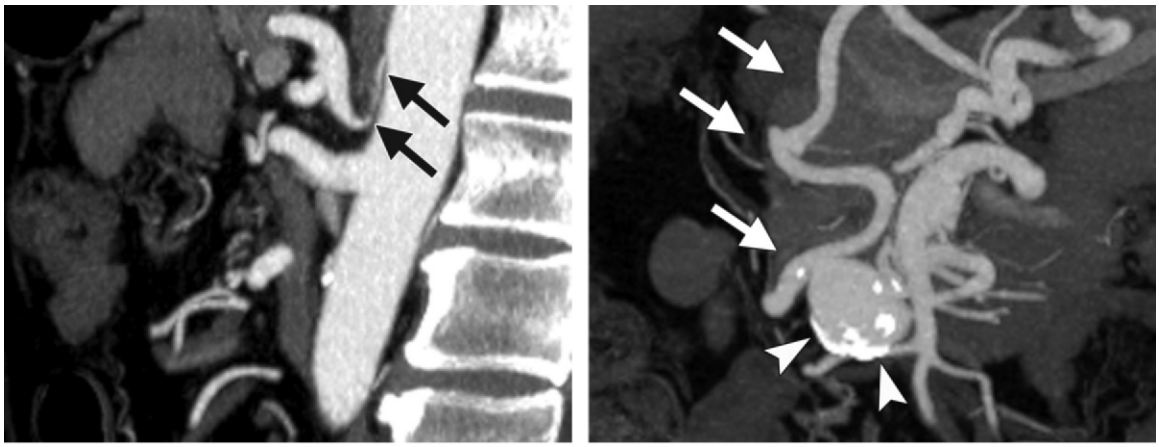

a. b.

Figure 3. MALS in a 67-year-old man with chronic abdominal pain. **(a)** Midline sagittal reformatted MIP image from an abdominal CT angiographic study in inspiration shows severe (>90%) nonatherosclerotic narrowing of the proximal celiac artery (arrows) with a characteristic hooked appearance. **(b)** Coronal oblique MIP image shows a tortuous and hypertrophied pancreaticoduodenal collateral vessel (arrows) and a 3-cm true aneurysm in the pancreaticoduodenal arcade (arrowheads).

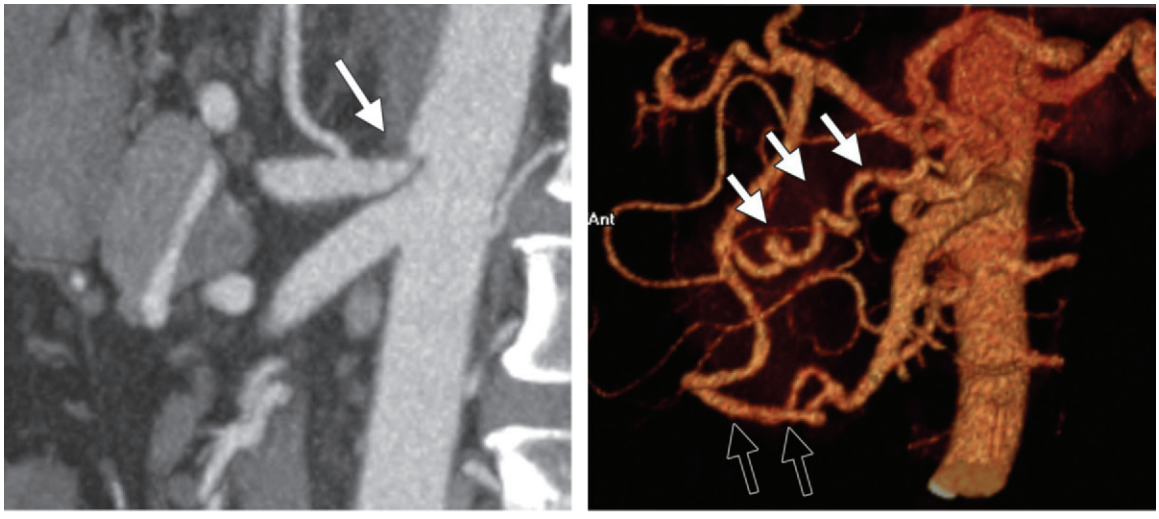

a. b.

c.

Figure 4. Incidentally detected proximal celiac stenosis in a 50-year-old man with advanced liver disease who was being evaluated for hepatocellular carcinoma. **(a)** Midline sagittal reformatted MIP image from an abdominal CT angiographic study shows an indentation on and moderate narrowing of the proximal celiac artery (arrow) caused by the median arcuate ligament. **(b)** Three-dimensional VR image shows a large, tortuous collateral vessel between the gastroduodenal branch of the celiac trunk and the splenic artery (white arrows). A large celiac artery–SMA pancreaticoduodenal collateral vessel is also present (black arrows). **(c)** Axial CT image at the level of the celiac artery origin shows a patent proximal celiac artery. The proximal narrowing is very difficult to appreciate on axial images (as seen in this case) and can easily be missed if sagittal reformatted images are not reviewed.

changes in the adjacent aorta and proximal celiac segment, helps distinguish MALS from atherosclerotic narrowing. Poststenotic dilatation may be present in severe stenosis, and, in some cases, hemodynamic compensation can be seen in the form of collateral vessels between branches of the celiac axis and the SMA, usually via the pancreaticoduodenal arcade. These collateral vessels can be tortuous and prominent, and hemodynamic effects can induce the formation of aneurysms in the pancreaticoduodenal arcade (Fig 3) (9).

Catheter angiography was used in the past for the diagnosis of MALS but has been superseded by multidetector CT, which provides an excellent 3D overview of the vascular anatomy in these patients. At CT or MR angiography, the characteristic finding of proximal celiac narrowing may not be appreciated on axial images. This narrowing is best visualized on sagittal MIP reconstructed images (Fig 4). Abdominal CT is typically performed in inspiration, and proximal celiac narrowing caused by the median arcuate ligament is reported to be more common and pronounced in expiration. Therefore, we perform CT angiography for suspected MALS in both deep inspiration and deep expiration, thereby allowing a comprehensive evaluation of the dynamic changes in celiac artery diameter with respiration. Two CT angiographic acquisitions through the proximal abdominal aorta are obtained rapidly and back-to-back during a single injection of contrast material, with a short pause to allow the change in breathing. To obtain two CT angiographic acquisitions in a short time, we perform the examination on multidetector CT scanners with 64 or more detector rows at a pitch ranging from 1.0 to 1.5, with the injection of 125 mL of a high concentration of contrast agent (iohexol [Omnipaque 350; GE Healthcare, Princeton, NJ]) at a rate of 4 mL/sec. Sagittal and coronal images are reconstructed in both phases. Duplex US is occasionally performed for suspected MALS. Flow velocities are evaluated during both inspiration and expiration. The diagnosis of MALS may be suggested if a marked increase in flow velocity occurs in the celiac artery in end expiration (10). It is important to note that the radiologic finding of celiac compression alone is not sufficient to make the diagnosis of MALS, unless hemodynamic alterations and clinical symptoms are also present (Fig 5).

Figure 5. Incidentally detected proximal celiac artery narrowing in a 76-year-old woman who was undergoing CT for surveillance of an abdominal aortic aneurysm. Midline sagittal reformatted MIP image from an abdominal CT angiographic study in inspiration shows significant stenosis of the proximal celiac artery (arrow) with poststenotic dilatation. Given the absence of any atherosclerotic changes in the proximal celiac artery, this stenosis can be attributed to compression by the median arcuate ligament. However, because the patient did not have any clinical signs or symptoms of MALS, this finding represents only physiologic compression of the artery, not the syndrome.

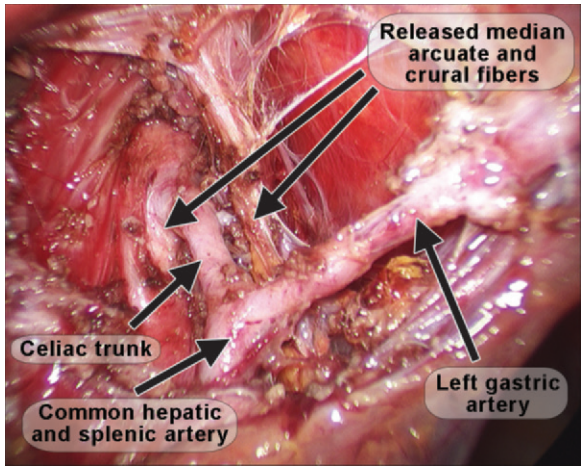

Figure 6. Surgical release of the fibers of the median arcuate ligament in a 28-year-old man with MALS. Photograph obtained during laparoscopic surgery shows the released fibers of the median arcuate ligament in the vicinity of the celiac artery and its branches.

Treatment

There is no consensus on the management of suspected MALS, and surgical treatment remains controversial. Successful surgical intervention for MALS depends on accurate diagnosis and appropriate patient selection. Younger patients with symptoms of postprandial pain and weight loss of more than 20 pounds are more likely to benefit from surgery (11). The treatment of MALS

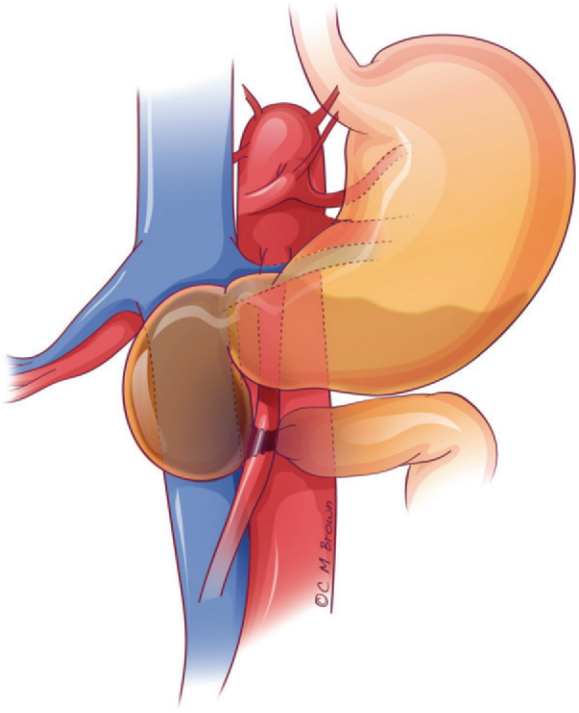

Figure 7. Drawing illustrates SMA syndrome, with compression of the mid-transverse duodenum between the proximal SMA and the aorta, resulting in proximal duodenal and gastric dilatation.

remains mainly surgical, involving transection of the median arcuate ligament, often in conjunction with some form of surgical celiac reconstruction, bypass surgery, or endovascular stent placement (Fig 6) (12–14). Laparoscopic approaches (either transabdominal or retroperitoneal) have recently replaced open surgical procedures (12–14). Endovascular therapy alone does not have a role as a primary intervention for MALS (12–14). Endovascular coil embolization is the preferred treatment for pancreaticoduodenal aneurysms (9). Because outcomes following surgery remain variable, some surgeons question whether MALS represents a true clinical entity (15).

SMA Syndrome

Originally described by Rokitansky in 1861, SMA syndrome (also known as cast syndrome and arteriomesenteric duodenal compression syndrome) consists of obstruction of the third portion of the duodenum due to compression between the SMA and the aorta (Fig 7) (16). Wilkie (17) described this condition in 1927 as a chronic duodenal ileus, and his name is occasionally used eponymously. SMA syndrome is a rare cause of proximal duodenal obstruction.

Anatomy and Pathogenesis

The SMA arises at the L1-2 level and courses anteriorly and inferiorly, forming an angle with the aorta known as the AMA. The third portion of the duodenum crosses between the aorta and the proximal SMA at approximately the L3 level. Normally, the third portion of the duodenum is surrounded by retroperitoneal fat, which provides a "cushion" for the duodenum between the anterior SMA and posterior aorta and helps maintain a wide AMA and AMD. Thus, it would seem intuitive that it is not the total body fat, but rather the intraabdominal fat—specifically, the retroperitoneal fat in the mesenteric root—that would be the key factor in maintaining a wide AMA and AMD. Various studies have reported the normal range of the AMA and AMD to be 28°–65° and 10–34 mm, respectively (Fig 8) (18–21).

SMA syndrome occurs in the following scenarios:

1. Conditions associated with rapid and severe weight loss, resulting in a loss of retroperitoneal fat, with resulting decreases in AMA and AMD and duodenal compression. These conditions include wasting conditions such as acquired immunodeficiency syndrome, malabsorption, cancer, and other conditions associated with cachexia; catabolic conditions such as burns and major surgery; eating disorders (eg, anorexia nervosa); drug abuse; and conditions following weight loss–related surgeries (eg, bariatric surgery) (22,23).
2. Patients who have undergone corrective surgery for scoliosis, in whom lengthening of the spine is postulated to increase tension on the mesentery and thus decrease AMA and AMD (24,25).
3. Conditions involving applied external abdominal pressure such as from a body or hip spica cast (26).
4. Anatomic variants such as an insertional variation of the ligament of Treitz or low origin of the SMA, which may result in a more cranial disposition of the duodenum into the acute vascular angle between the aorta and proximal SMA (23,27).

Because SMA syndrome occurs relatively infrequently, its exact prevalence in the general population is extremely difficult to measure, although it has been estimated to be 0.1%–0.3% on the basis of gastrointestinal barium studies (18). However, in patients with scoliosis who undergo corrective spinal surgery, a prevalence of up to 2.4% has been reported (28).

Clinical Presentation

Females are more commonly affected by SMA syndrome, with two-thirds of patients being between 10 and 39 years of age (23). Symptoms include postprandial epigastric pain and fullness, nausea, vomiting, weight loss, and anorexia. The pain may classically be relieved by lying in the prone or left lateral decubitus position (18,22,23). The vomiting and weight loss

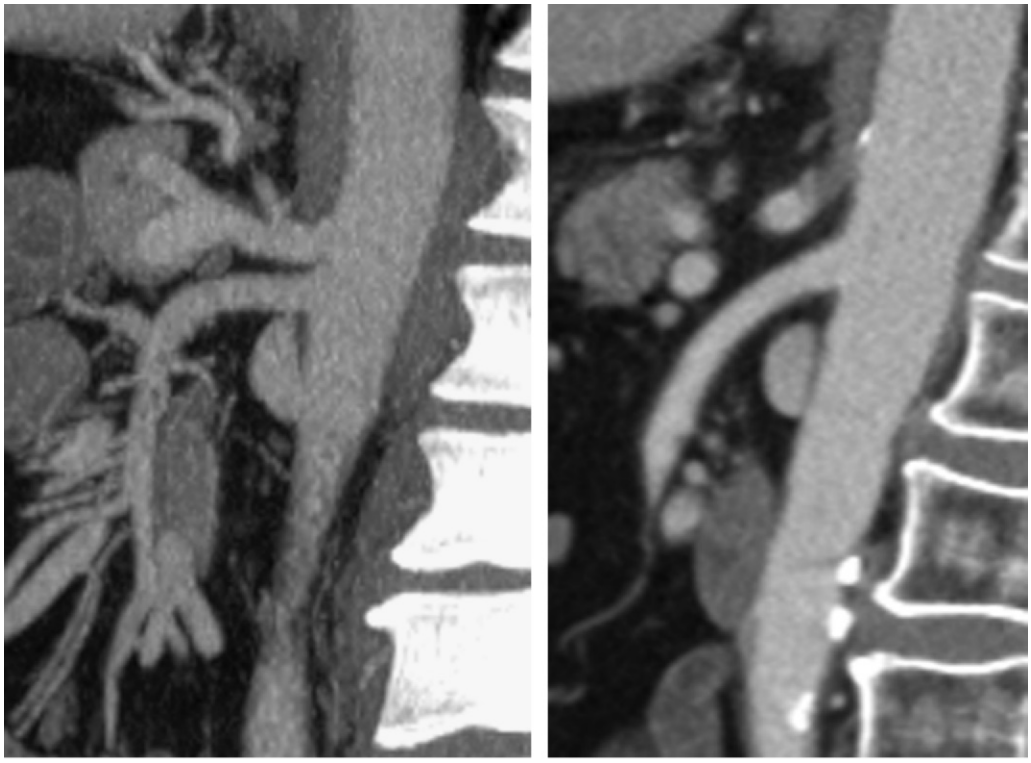

a. b.

Figure 8. Midline sagittal reformatted MIP images from two different abdominal CT studies demonstrate the normal AMA (>30°) **(a)** and AMD (>10 mm) **(b)**.

result in a self-perpetuating cycle with further loss of retroperitoneal fat. Patients may also complain of severe reflux, and endoscopy may demonstrate severe esophagitis and gastritis associated with stasis and chronic obstruction (22). All other causes of duodenal obstruction, whether intrinsic (benign or malignant strictures and tumors) or extrinsic (eg, tumors, aneurysm, pancreatitis), must be excluded with imaging or upper endoscopy before a diagnosis of SMA syndrome is made.

Radiologic Findings

Traditional imaging methods for diagnosis include an upper gastrointestinal barium study and conventional mesenteric angiography (18,20), which only allow evaluation of the gastrointestinal tract and vascular anatomy, respectively. Barium studies show a dilated stomach and proximal duodenum, a vertical extrinsic impression on the third portion of the duodenum resulting from its compression, antiperistaltic waves proximal to the obstruction, delayed gastroduodenal emptying, and relief of obstruction with postural change (Fig 9) (20,29). In severe cases, barium may fail to pass through the obstructed duodenum. Mesenteric angiography shows acute angulation of the SMA and a reduced AMD. The AMA and AMD in patients with SMA syndrome have been reported to be 6°–22° and 2–8 mm, respectively (19,22,29–32). In a recent multidetector CT study of four cases of SMA syndrome, the mean AMA and AMD were 13.5° and 4.4 mm, respectively (18).

CT performed after the injection of iodinated contrast material allows simultaneous evaluation of the mesoaortic vascular anatomy, transverse duodenal compression, and proximal dilatation, and is thus the diagnostic test of choice for SMA syndrome (Figs 9, 10) (18,19). CT is best performed in the late angiographic phase to allow simultaneous optimal depiction of the vascular anatomy and the bowel wall. Use of positive oral contrast agent may be avoided in patients with severe obstruction. Sagittal MPR images are needed to evaluate the AMA. CT has the added advantage of showing the exact anatomic position of the duodenum in the vascular angle and excluding other causes of obstruction. However, SMA syndrome should not be diagnosed solely on the basis of CT findings of a reduced AMA and AMD in the absence of any signs or symptoms of duodenal obstruction (Fig 11).

Treatment

For acute and initial presentations, treatment is usually conservative, consisting of fluid and electrolyte resuscitation, nasojejunal feeding to bypass the obstruction, small liquid meals, and

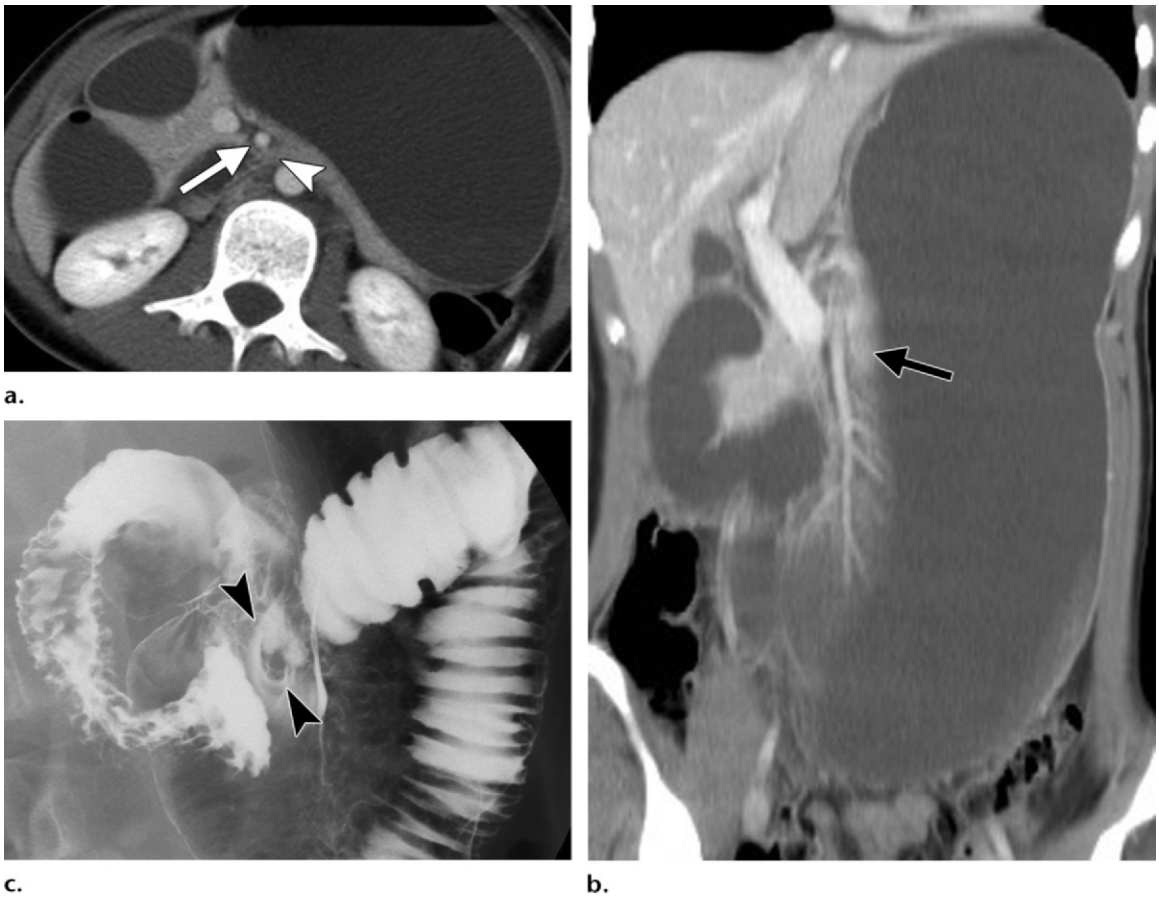

Figure 9. SMA syndrome in a 23-year-old woman with an inability to gain weight due to a chronic fear of eating and a 1-year history of increasing abdominal pain. **(a)** Axial CT image shows severe compression of the mid-transverse duodenum (arrowhead) in the narrowed space between the SMA (arrow) and the aorta. Note the absence of retroperitoneal fat. **(b)** Coronal reformatted image shows a massively dilated stomach and proximal duodenum. The SMA is seen crossing anterior to the point of transition at the mid-transverse duodenum (arrow). **(c)** Image from an upper gastrointestinal barium study shows a characteristic extrinsic impression on the mid-transverse duodenum (arrowheads) caused by the overlying SMA.

mobilization of the patient into the prone or left lateral decubitus position. Nutritional support with peroral or parenteral hyperalimentation may also be included and is aimed at restoration of retroperitoneal fat and weight gain, which can relieve some symptoms (18,22,23,30).

Surgical treatment is indicated if conservative management fails and usually involves bypassing the obstructed segment. Surgical options include duodenojejunostomy, gastrojejunostomy, or lysis of the ligament of Treitz with derotation of the bowel (Strong procedure) (18,22,23,30). Although the data available in the literature do not provide enough statistical evidence to identify any surgical procedure as superior, laparoscopic duodenojejunostomy currently seems to be the favored procedure (33).

May-Thurner Syndrome

May-Thurner syndrome, also known as iliac vein compression syndrome and Cockett syndrome (34,35), consists of obstruction of the left CIV caused by the crossing right common iliac artery (CIA) (Fig 12). The resultant chronic venous stagnation results in chronic left lower extremity swelling with or without thrombosis of the left iliac and femoral veins. May-Thurner syndrome is named after the Austrian surgeon and pathologist who, in 1957, described the formation of an endovascular "spur" in the proximal left CIV in cadaver dissections (36).

Pathogenesis

Two factors are thought to contribute to the partial venous obstruction in May-Thurner syndrome: *(a)* extrinsic factors causing physical compression of the left CIV between the right CIA and the underlying vertebral body, and *(b)* intrinsic factors resulting from formation of internal webs or bands (spurs) secondary to local intimal hypertrophy due to the chronic pulsatile force of the overlying right CIA (34,36).

The true prevalence of May-Thurner syndrome is unknown. The incidence of venous

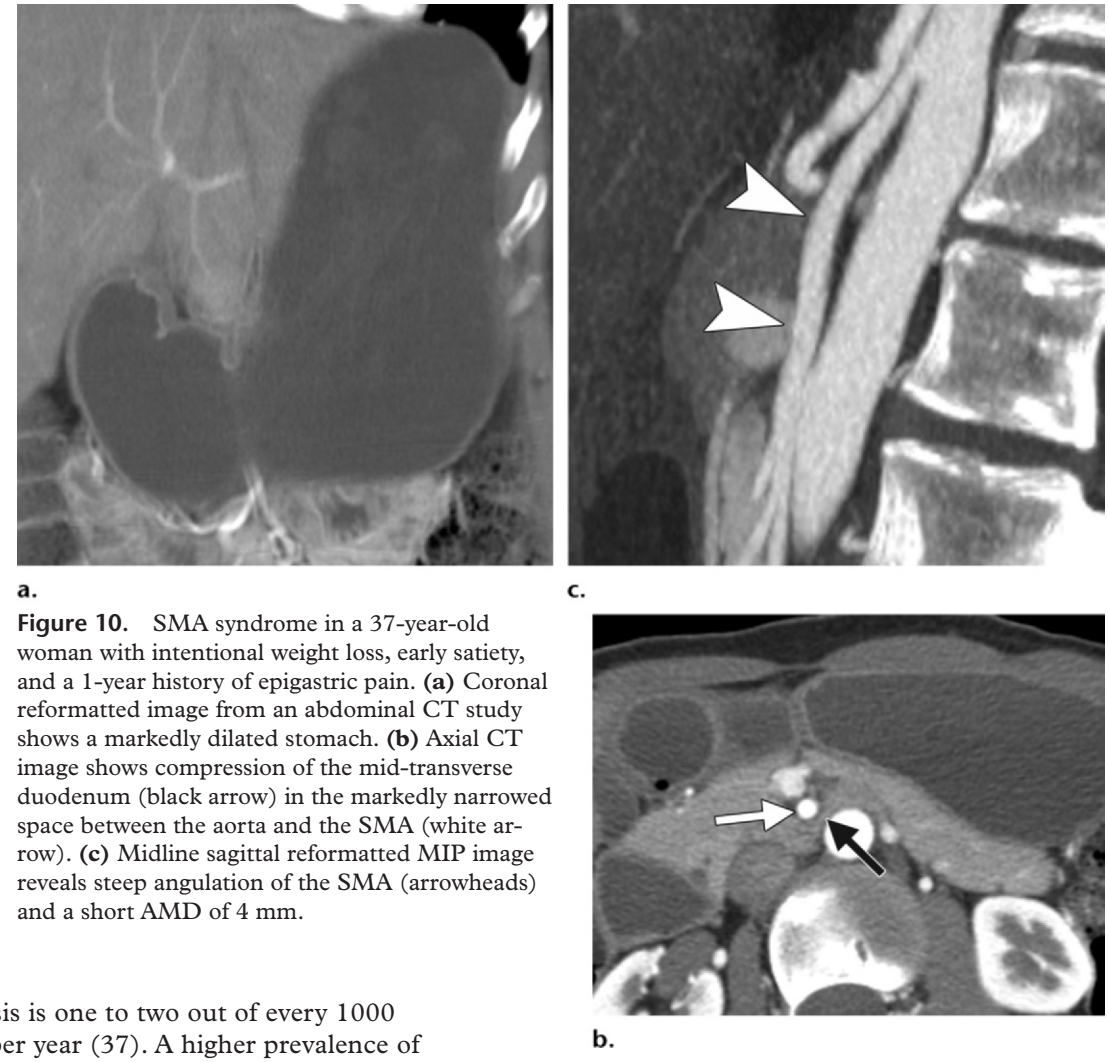

Figure 10. SMA syndrome in a 37-year-old woman with intentional weight loss, early satiety, and a 1-year history of epigastric pain. **(a)** Coronal reformatted image from an abdominal CT study shows a markedly dilated stomach. **(b)** Axial CT image shows compression of the mid-transverse duodenum (black arrow) in the markedly narrowed space between the aorta and the SMA (white arrow). **(c)** Midline sagittal reformatted MIP image reveals steep angulation of the SMA (arrowheads) and a short AMD of 4 mm.

thrombosis is one to two out of every 1000 persons per year (37). A higher prevalence of thrombosis in the left leg (~60% of cases) than in the right leg (~40%) has been reported (37). May and Thurner (36) found a spurlike projection in the proximal left CIV in 22% of 430 cadavers. In later studies, the prevalence of venous spurs has been reported to be 49%–62% in patients with left iliofemoral thrombosis (38). Therefore, May-Thurner syndrome should be relatively common, and there should be a high degree of suspicion, particularly in young women who present with acute iliofemoral thrombosis of the left leg. Because typical risk factors for deep venous thrombosis include surgery, injury, pregnancy, and oral contraceptive use, May-Thurner syndrome is commonly overlooked in the differential diagnosis, particularly if patients have other risk factors.

Clinical Presentation

May-Thurner syndrome generally affects young and middle-aged people and is more common in women (34,39). Iliocaval compression may be asymptomatic (36); the typical symptom (when present) is left lower extremity swelling, which may manifest acutely due to left-sided iliofemoral vein thrombosis or may be chronic due to venous congestion without underlying thrombosis. Other chronic symptoms include varicosities and chronic venous stasis ulcers. Serious complications such as pulmonary embolism or phlegmasia cerulea dolens can result. Phlegmasia cerulea dolens represents a rare and grave sequel of extensive iliofemoral vein thrombosis that is characterized by acute limb ischemia, which can progress to gangrene.

Radiologic Findings

Traditionally, ascending iliac contrast venography has been performed for diagnosis; this procedure demonstrates the venous compression and allows hemodynamic evaluation by measuring pressure gradients (34). An additional and important diagnostic finding is the presence of tortuous venous collateral vessels crossing the pelvis to join the contralateral veins. However, venography is invasive and time consuming and can result in postprocedural phlebitis. Furthermore, it cannot be performed in patients with extensive iliofemo-

Figure 11. Short AMD in a 38-year-old woman who was undergoing CT for abdominal pain following exploratory laparoscopy for endometriosis. Midline sagittal reformatted image shows a short AMD (arrowheads) and steep SMA angulation. The patient demonstrated no evidence of duodenal obstruction at CT and no clinical signs or symptoms of SMA syndrome.

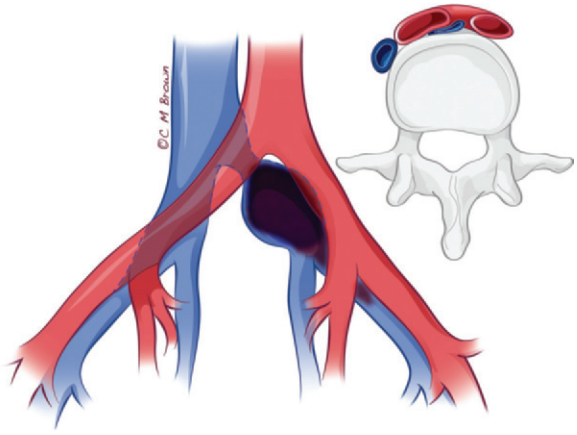

Figure 12. Drawing illustrates May-Thurner syndrome, showing compression of the left CIV between the right CIA and the anterior surface of the underlying vertebral body, resulting in left pelvic and lower extremity venous congestion.

ral vein thrombosis. Duplex US is limited in the identification of abnormalities of the iliac veins because these veins lie deep in the pelvis and are commonly obscured by bowel gas. More recently, the use of multidetector CT or MR venography has been advocated for diagnosis (40–42). However, MR venography is expensive, time consuming, and difficult to perform in acutely ill patients. Multidetector CT performed in the pelvic venous phase after the injection of iodinated contrast material reliably shows the iliac vein compression, which is best seen in the transverse plane (40). CT can also show the extent of iliofemoral vein thrombosis (if present) and help exclude other causes of venous compression such as pelvic masses (Fig 13).

Treatment

Treatment is aimed at relieving the mechanical obstruction and should ideally be performed before the onset of deep venous thrombosis and venous insufficiency syndrome. Catheter-directed thrombolysis has been shown to have a much higher venous patency rate at 6 months compared with systemic anticoagulation alone, which is no longer used due to its low patency rate (43). A thrombosis recurrence rate of 73% has been reported in cases in which the mechanical obstruction is not addressed (38). Catheter-directed thrombolysis followed by endovascular stent placement has a high success rate (95%) and is now the preferred management technique (Fig 14) (39,44). Excellent 1-year patency rates of 90%–100% (mean, 96%) following successful stent placement have been reported (39). Oral anticoagulants are used following stent placement to prevent the recurrence of thrombosis (39). Surgical approaches such as vascular transposition, venous bypass surgery, and excision of intraluminal bands with venoplasty have also been advocated and successfully used (39,45,46).

Nutcracker Syndrome

The term *nutcracker phenomenon* refers to the anatomic compression of the LRV that can occur between the SMA and the aorta (“anterior nutcracker”) or, if the LRV has a retroaortic or circumaortic course, between the aorta and an underlying vertebral body (“posterior nutcracker”). In 1937, Grant (47) described the position of the LRV between the aorta and SMA as being akin to that of a nut between the jaws of a nutcracker. However, the nutcracker phenomenon is not always associated with clinical symptoms. Nutcracker syndrome is rare and refers to the symptom complex that develops due to increased venous pressure in the LRV secondary to obstruction of its venous outflow into the inferior vena cava (IVC). This results in the development of intra- and extrarenal hypertensive valveless venous collateral vessels—most often on the left side—or gonadal vein reflux. Although the first clinical report of this syndrome was made by El-Sadr and Mina in 1950 (48), the term *nutcracker syndrome* was first used by de Schepper in 1972 (49,50).

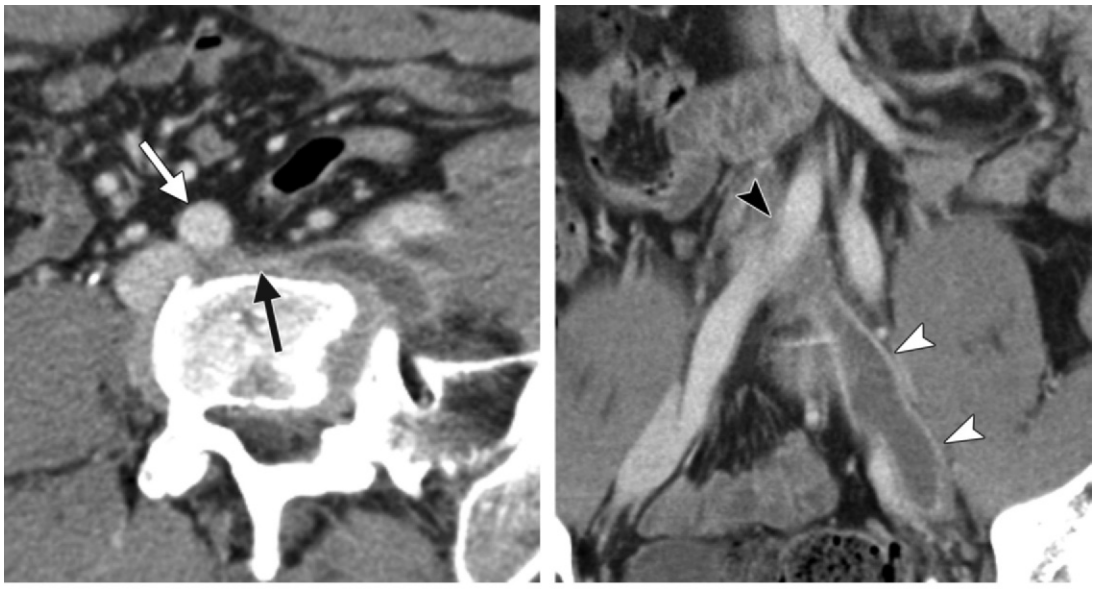

a. b.

Figure 13. May-Thurner syndrome in a 45-year-old man who presented with acute left lower extremity pain, swelling, and skin discoloration following a long-distance flight. **(a)** Axial CT image of the pelvis shows severe compression of the left CIV (black arrow) between the right CIA (white arrow) and the underlying vertebral body. **(b)** Coronal reformatted image shows the overriding right CIA (black arrowhead) with acute extensive thrombosis and dilatation of the external iliac vein (white arrowheads).

Pathogenesis

Steep angulation of the SMA relative to the aorta resulting in a short AMD can predispose to nutcracker syndrome (Fig 15) (50,51). Thus, anterior nutcracker syndrome may occur simultaneously with SMA syndrome. An association with a thin or asthenic body habitus has long been noted. Conceivably, all conditions that result in rapid weight loss and loss of retroperitoneal fat can predispose to nutcracker syndrome. It stands to reason that an AMA and AMD that can result in SMA syndrome would be enough to cause LRV compression as well. A significantly decreased AMD of 3 mm has been reported in patients with nutcracker syndrome, compared with a range of 10–14 mm in the control group (52). Similarly, an AMA of less than 16° has been reported in patients with nutcracker syndrome (53). Positional factors and other anatomic variants such as an abnormally high course of the LRV have also been postulated to cause LRV compression (51). Compression of the LRV from tumors or masses in the retroperitoneum should not be considered as representing true nutcracker syndrome. Because of the large increase in the number of abdominal CT examinations in the past decade, asymptomatic narrowing of the LRV between the aorta and SMA with or without retrograde venous congestion is occasionally seen as an incidental finding in patients undergoing CT for unrelated reasons.

Teaching Point

Clinical Presentation

Because of the variability of symptoms and the absence of consensus regarding diagnostic criteria, the exact prevalence of nutcracker syndrome is unknown. The majority of affected patients are young or middle aged, and nutcracker syndrome is slightly more common in females.

No consensus exists as to what symptoms are severe enough to warrant the designation of a clinical syndrome, and the diagnosis is often overlooked and delayed. Symptoms result from increased pressure in the LRV, vary widely from mild to severe, and may be exacerbated by physical activity. Manifestations include mild microhematuria to severe gross hematuria (which can result in anemia), mild to severe orthostatic proteinuria, and left flank pain secondary to the passage of ureteral blood clots. Massive gonadal vein reflux may result in left-sided varicoceles in males and left-sided vulvar and pelvic varices in females. Symptoms of pelvic venous congestion (chronic pelvic pain, dyspareunia, dysuria, and dysmenorrhea) may occur in females (49,54–56). The most common symptom is hematuria resulting from the rupture of fragile varices into the collecting system. Conversely, nutcracker syndrome remains a very rare cause of hematuria.

Radiologic Findings

Multidetector CT or MR imaging performed in the venous phase after the injection of iodinated contrast material allows simultaneous depiction

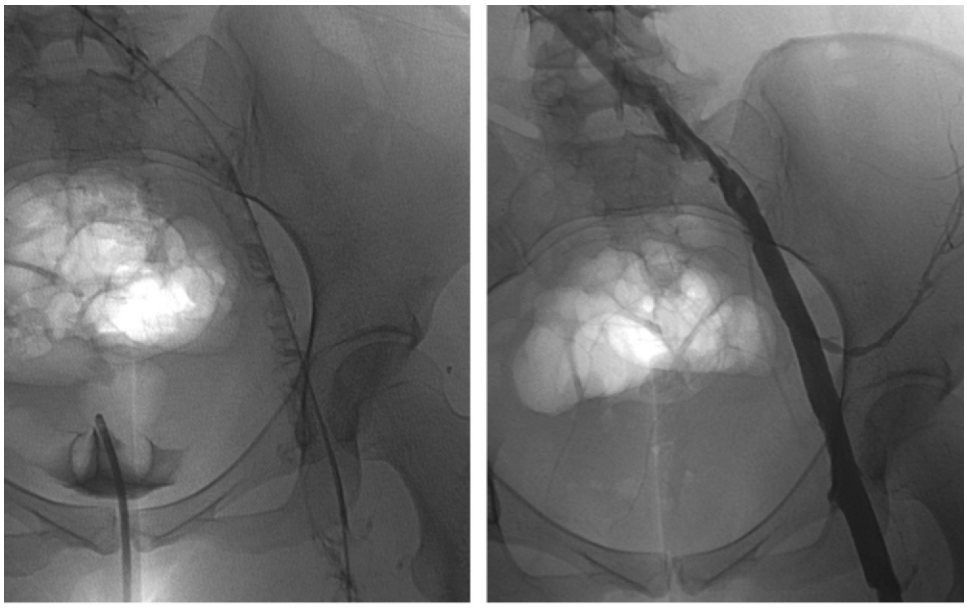

a. b.

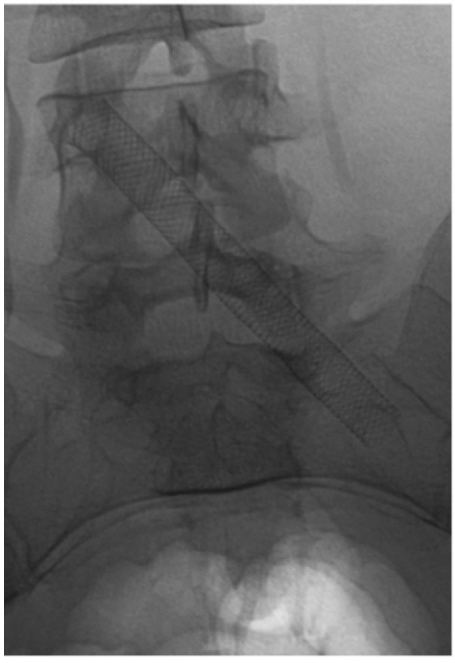

c.

Figure 14. Endovascular treatment for May-Thurner syndrome in a 40-year-old woman. **(a)** Ascending venogram obtained prior to tissue plasminogen activator (TPA) infusion shows an extensive thrombus in the left common and external iliac veins that extends into the proximal femoral vein. **(b)** Repeat ascending venogram obtained 24 hours after TPA infusion shows significant clot dissolution throughout the occluded segments. **(c)** Digital spot radiograph shows a stent that was placed in the left CIV following thrombolysis.

of the mesoaortic anatomy and focal midline compression of the LRV and its hemodynamic consequences (prestenotic dilatation; hilar, periureteric, and pelvic varices; dilated gonadal veins) (Fig 16). Sagittal MPR images allow evaluation of the AMA and AMD, and coronal MPR images best depict the varices and dilated gonadal veins. In the multidetector CT era, IVU is no longer performed for suspected nutcracker syndrome. Excretory or retrograde urography may show indentations and scalloping of the renal pelvis or ureter by enlarged retroperitoneal varices.

Duplex US can provide hemodynamic information in these patients. A significantly higher ratio of peak systolic velocity at the point of renal vein compression to peak systolic velocity in the hilar renal vein has been reported in patients with nutcracker syndrome compared with asymptomatic control subjects (56,57). A peak systolic velocity ratio of over 4.7 has been reported to have a sensitivity of 100% and a specificity of 90% for the diagnosis (58). Transvaginal US can show the extent of pelvic varices in patients with symptoms of pelvic congestion.

The definitive diagnostic test for nutcracker syndrome remains retrograde venography, which allows both determination of the renocaval pressure gradient and contrast mapping of the dilated gonadal vein and the perihilar, periureteral, and pelvic collateral network. The LRV-to-IVC pressure gradient is less than 1 mm Hg in healthy subjects (59). A gradient of over 3 mm Hg has been reported to be hemodynamically significant in patients with LRV compression, although a wide range of gradient values has been published (50,60). Notably, nutcracker syndrome remains a clinical diagnosis and should be made only when characteristic symptoms are present. Observations of LRV compression at

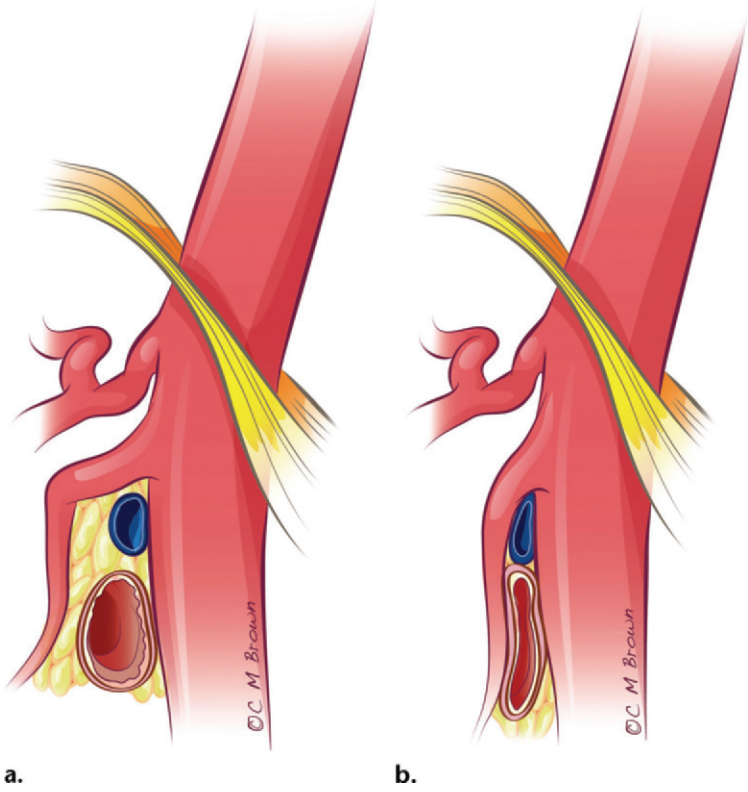

Figure 15. Relationship between the LRV and the duodenum in the angle between the aorta and the SMA. **(a)** Drawing illustrates a normal AMA and AMD, which are promoted by the presence of retroperitoneal fat in the angle. **(b)** Drawing illustrates compression of both the LRV and the duodenum when the AMD is decreased, with an associated decrease in the AMA.

multidetector CT or MR imaging in the absence of varices and symptoms merely represent the nutcracker phenomenon, not nutcracker syndrome (Fig 17).

Treatment

Expectant treatment is preferred in younger or thin patients, or in those with mild symptoms. In patients younger than 18 years of age, symptoms generally resolve within 2 years as retroperitoneal fat increases and the AMD widens. Intervention is indicated in severely symptomatic patients. The primary goal is to alleviate LRV outflow obstruction and hypertension. Numerous surgical approaches such as LRV transposition to the more inferior IVC, external venous stent placement, LRV bypass surgery, renal autotransplantation to the iliac fossa, and left nephrectomy have been used (50,55,60). Gonadocaval bypass surgery with ligation or embolization of varices may be beneficial in patients with symptomatic pelvic varices. Endovascular LRV stent placement (Fig 18) has only recently been advocated, so that no long-term studies are yet available to help assess outcomes. However, stent migration, intimal fibromuscular hyperplasia, in-stent stenosis, and venous thrombosis are potential complications (50,60).

UPJ Obstruction by Crossing Vessels

UPJ obstruction implies a congenital partial obstruction (either functional or anatomic) at the junction of the renal pelvis and proximal ureter. This condition has an unclear natural history and, if left untreated, will result in symptoms, renal damage, or both.

Pathogenesis

UPJ obstruction is seen in approximately one out of every 20,000 live births (61). The prevalence of UPJ obstruction is less well defined in adults than in children. Furthermore, controversy exists regarding the cause of UPJ obstruction. Several causes have been postulated, including crossing vessels, an aperistaltic ureteral segment, an intrinsic luminal narrowing (in the form of stenosis

Figure 16. Nutcracker syndrome in a 22-year-old woman with progressive left lower quadrant pain and flank pain, as well as microscopic hematuria. **(a)** Axial CT image shows severe compression of the LRV (arrowhead) between the SMA (arrow) and the aorta. **(b)** Midline sagittal reformatted image shows steep angulation of the SMA (arrow) with compression of the LRV (arrowhead) in the narrowed aortomesenteric space. **(c)** Coronal reformatted image shows tortuous and dilated retroperitoneal varices (arrowheads) along the course of the left ureter. **(d)** Intravenous urographic (IVU) image shows multiple indentations on the left ureter (arrows) caused by retroperitoneal collateral vessels. **(e)** Axial CT image of the pelvis shows left-sided periuterine varices (arrow).

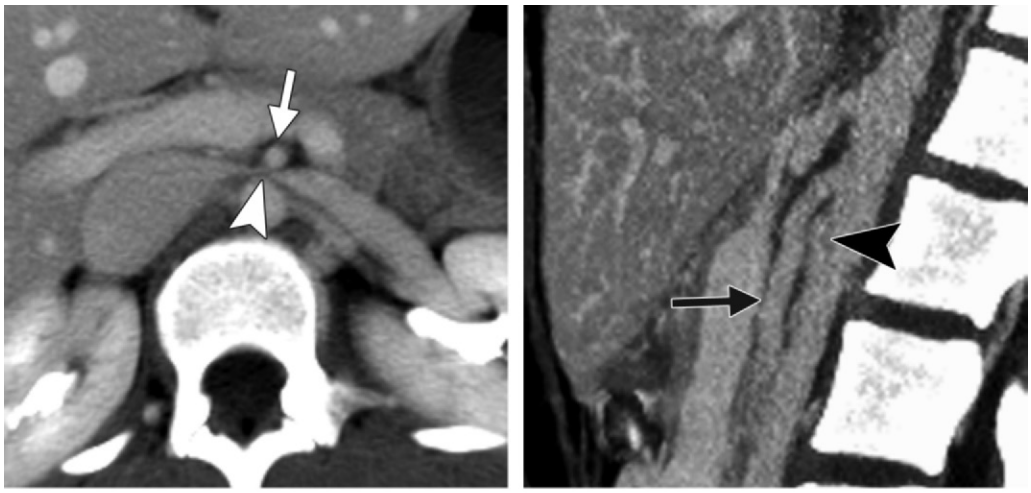

a.

b.

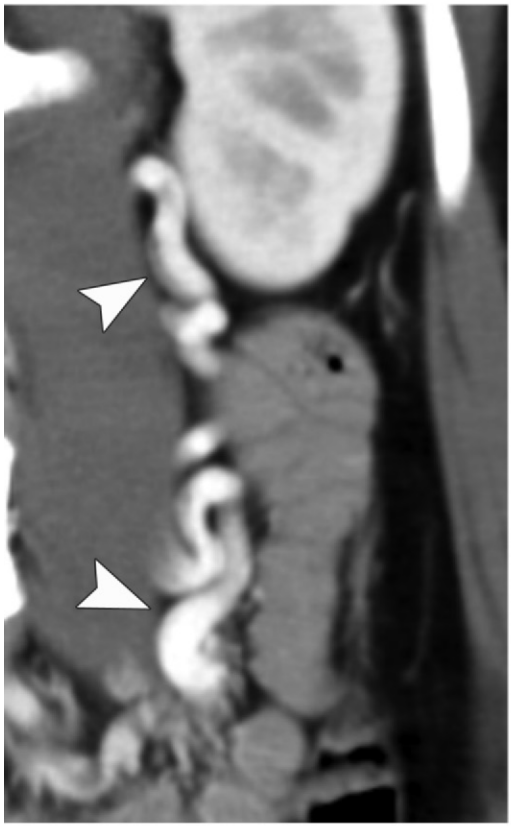

c.

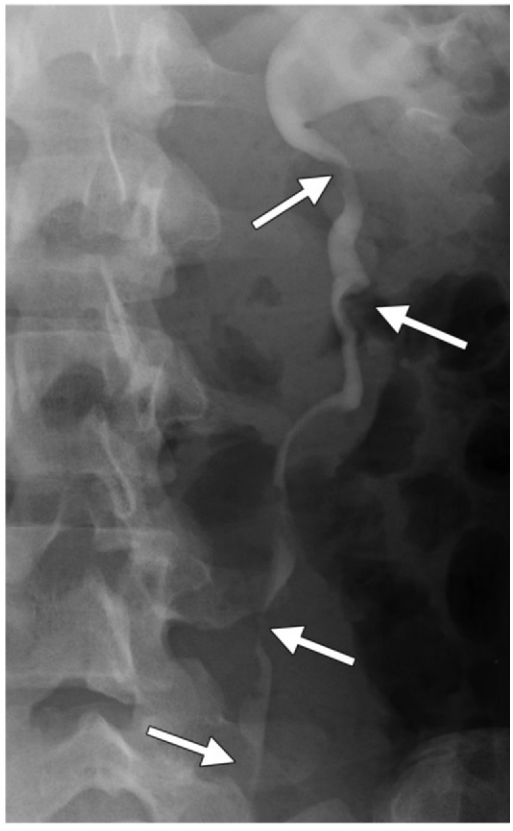

d.

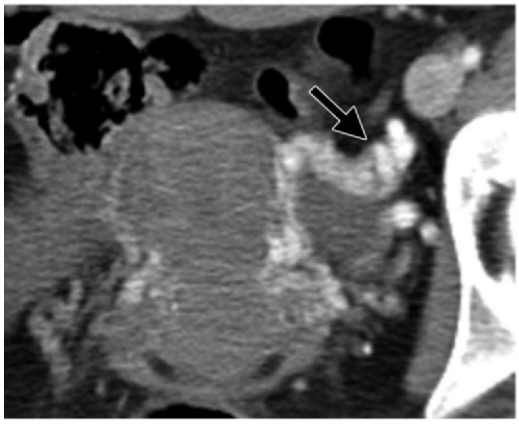

e.

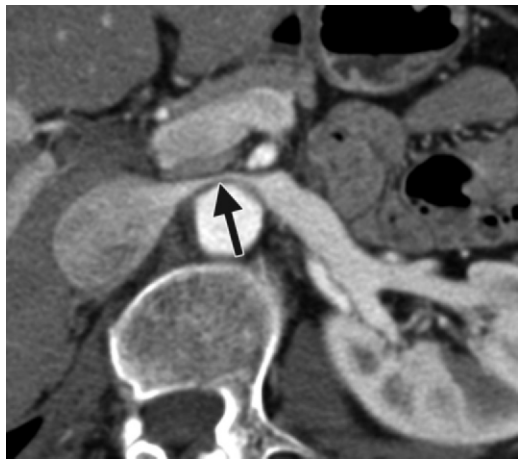

Figure 17. Incidentally detected LRV compression in a 53-year-old woman with chronic abdominal pain and weight loss. Urinalysis showed no evidence of gross or microscopic hematuria. Axial CT image shows marked narrowing of the LRV (arrow) as it courses between the superior mesenteric vessels and the abdominal aorta. The left gonadal and lumbar veins were of normal caliber, with symmetric perfusion of the kidneys. There was no evidence of left-sided renal hilar, retroperitoneal, or pelvic collateral vessels. These findings represent the nutcracker phenomenon, not nutcracker syndrome, given the absence of clinical signs and symptoms or hemodynamic effects resulting from the LRV compression.

or valves), excessive local collagen deposition, periureteral fibrosis (which may be secondary to recurrent urinary tract infection), and an insertional abnormality (which may be primary or develop over time as the renal pelvis distends) (62). In some cases, a specific cause for UPJ obstruction may not be detected. Additionally, causes may coexist and thus may be comitigating factors in the obstruction.

Of these causes, crossing vessels have received special attention, and their association with hydronephrosis has been known for over 100 years (63). A crossing vessel can be a renal artery or renal vein (or both) that crosses the ureteric transition point—most commonly, an anteriorly crossing artery. The lower pole segmental artery and vein in particular have been implicated in UPJ obstruction (Fig 19) (64). These vessels may be a branch of the main renal artery or vein or may arise separately (accessory branch) from the aorta, iliac artery, or IVC (Figs 20, 21). Crossing vessels have been implicated in 11%–79% of cases of UPJ obstruction (62,65–67). This wide reported range is likely due to the fact that any vessel that is present in the vicinity of the UPJ tends to be implicated as a cause of UPJ obstruction. However, only a vessel crossing immediately adjacent to the UPJ (within 1–2 cm) should be designated as a crossing vessel. One study found that in 43% of patients with UPJ obstruction due to a crossing vessel, no intrinsic abnormality was noted in the ureter at histologic analysis, thus implicating mechanical compression from crossing vessels as a direct pathogenetic mechanism of UPJ obstruction in selected cases (68). Conversely, crossing vessels have been reported in the setting of a normal UPJ in 19% of cases (67), and a high prevalence (71%) of crossing vessels has been reported in cadaveric studies (69). Furthermore, UPJ obstruction also occurs in the absence of crossing vessels (62). Thus, the causal relationship between crossing vessels and UPJ obstruction remains controversial, with ongoing debate as to whether these are causative, aggravating, or incidental factors.

Teaching Point

Clinical Presentation

UPJ obstruction may be detected in utero as well as in children or adults. Obstruction ranges from mild to severe and is generally slowly progressive. Early on, the obstruction may not be severe enough to cause symptoms or significant loss of renal function. Patients may present with flank pain, hematuria, renal stones, urinary tract infections, or pyelonephritis. Pain may be intermittent and may be related to the intake of large volumes of fluid or of fluids with a diuretic effect.

Radiologic Findings

Irrespective of the controversy regarding the role of crossing vessels in UPJ obstruction, their preoperative detection may be important to the urologist, since these vessels can be injured during therapeutic endopyelotomy and their presence may dictate the surgical approach that is used. Significant hemorrhage, pseudoaneurysms, or arteriovenous fistulas can result if these vessels are injured during surgery (70). Because renal arteries are end arteries, they must be preserved during surgery to prevent any loss of renal parenchyma, which can be significant if superimposed on preexisting decreased renal function.

Various imaging modalities have been used for the detection of crossing vessels. Catheter angiography is invasive and is limited for depicting the venous anatomy and the relationship of crossing vessels to the UPJ. IVU or retrograde urography may show an extrinsic impression at the UPJ. In the modern era of cross-sectional imaging, neither of these modalities is used for

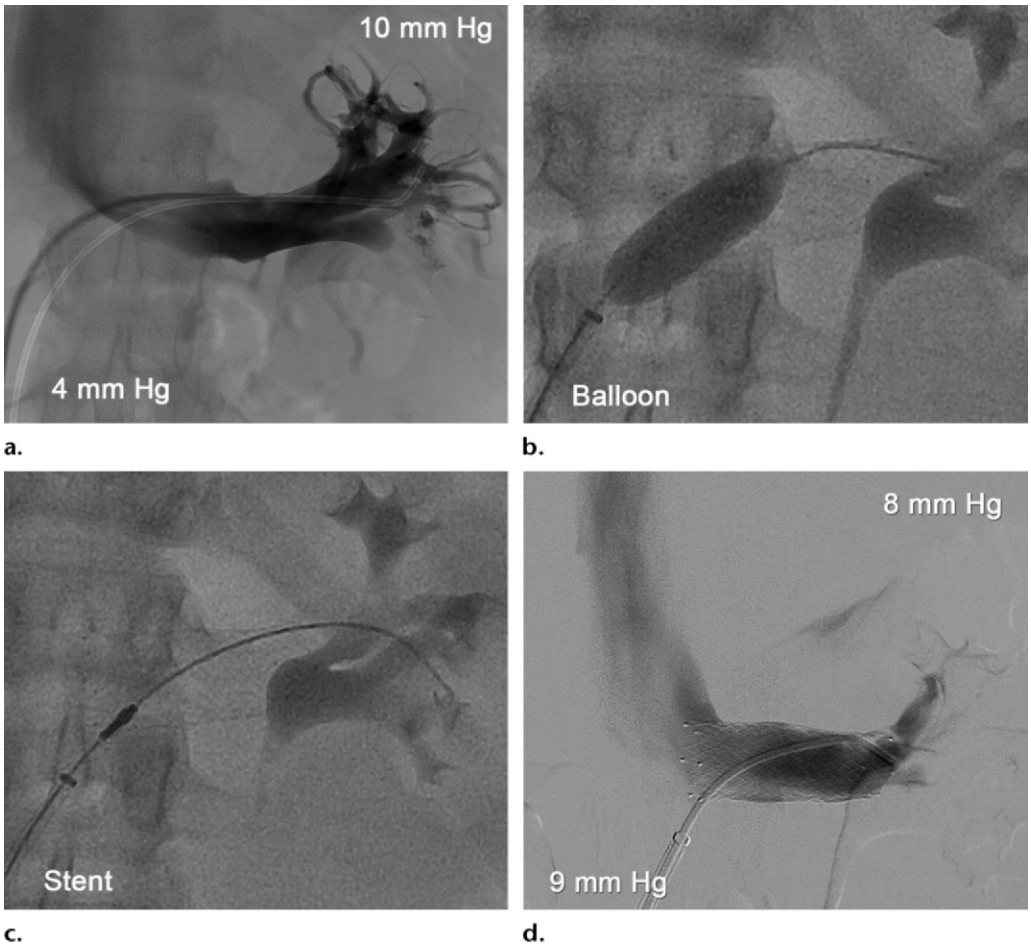

Figure 18. Nutcracker syndrome in a 17-year-old girl with a 2-year history of abdominal pain, gross hematuria, and proteinuria resulting in a hemoglobin level of 8.0 mg/dL. Results of cystoscopy confirmed the source of bleeding to be the left ureter. CT and duplex US helped confirm severe compression of the LRV between the SMA and aorta. Duplex US showed a marked increase in peak systolic velocity distal to the narrowing. **(a)** Direct left renal venogram shows a hemodynamically significant pressure gradient of 6 mm across the LRV (10 mm Hg in the LRV and 4 mm Hg in the IVC). **(b, c)** Spot radiographs depict placement of a stent across the stenotic segment of the LRV. **(d)** Postprocedural venogram shows restoration of a normal pressure gradient across the LRV (8 mm Hg in the LRV and 9 mm Hg in the IVC). Immediately following stent placement, the patient's abdominal pain and hematuria resolved completely. Postprocedural duplex US showed normalization of the velocities across the LRV.

the detection of crossing vessels. Duplex US performed after contrast material injection is more accurate in the depiction of crossing vessels than is routine duplex US (66), which does not have a high specificity and remains very operator dependent (71). US appears to be accurate only when an endoscopic (endoureteral) approach is used or contrast material is injected (66), with high accuracy reported for the latter (72,73). In a small series of pediatric patients, MR angiography was shown to be accurate for the detection of crossing vessels (74), but it remains limited by its high cost and lengthy examination time. Multidetector CT with user-defined MPR and 3D VR provides excellent depiction of crossing vessels, with a reported positive predictive value of 100% (Figs 20, 21) (75,76). Multidetector CT should be performed in the late arterial phase to allow identification of both arteries and veins.

Dilatation of the renal pelvis is a predominant feature of UPJ obstruction, with a variable amount of dilatation of the caliceal system. The distended renal pelvis in UPJ obstruction is largely extrarenal with a characteristic inverted "teardrop" morphology and generally "drapes" over a lower pole segmental vessel with the proximal ureter hooking over the vessel (Figs 19, 20). With use of multidetector CT, the relationship of the vessels to the ureteric transition zone and the severity and morphology of the hydronephrosis are easily depicted in a single examination.

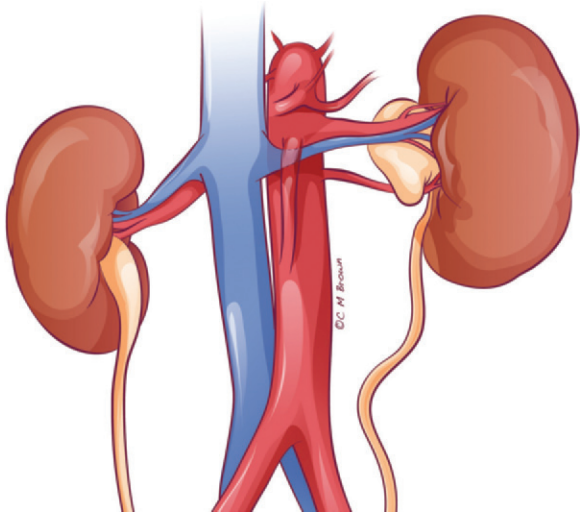

Figure 19. Drawing illustrates UPJ obstruction by a crossing lower pole segmental renal artery. Note how the ballooned extrarenal pelvis is draped over the crossing artery.

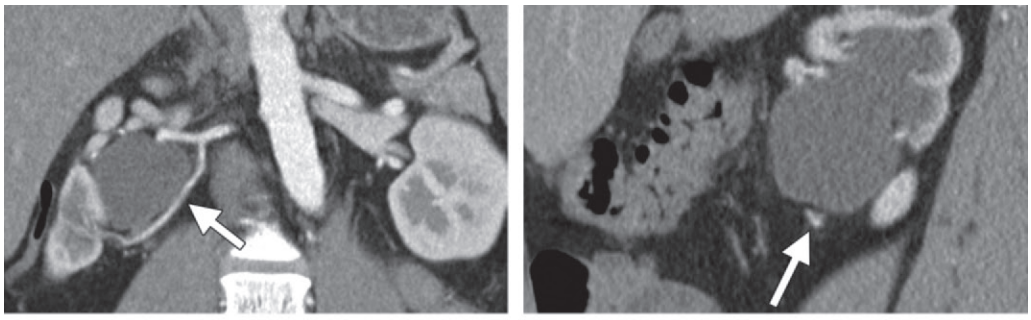

a. b.

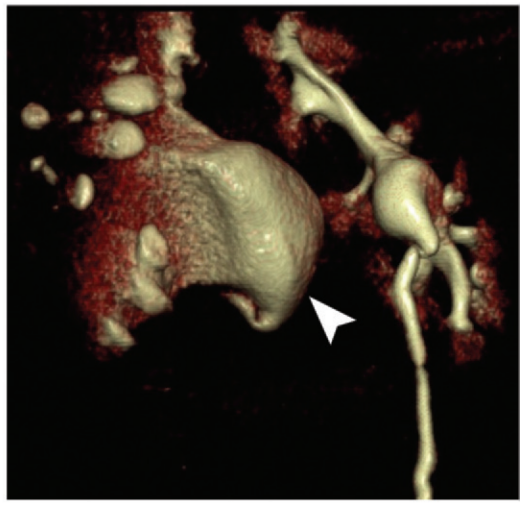

c.

Figure 20. UPJ obstruction in a 34-year-old man with right flank pain and hematuria. **(a)** Coronal reformatted image from a CT urographic study shows an early branching right lower pole segmental artery (arrow) crossing the ureteropelvic transition. **(b)** Sagittal reformatted image shows a markedly dilated renal pelvis and renal parenchymal atrophy. The crossing vessel is also seen (arrow). **(c)** Three-dimensional VR image shows greater dilatation of the renal pelvis (arrowhead) compared with the intrarenal calices, a characteristic finding in UPJ obstruction. Note also the hooked appearance of the proximal ureter as it crosses over the artery.

Treatment

Therapeutic intervention is largely based on symptoms, degree of hydronephrosis, and deterioration of renal function. Surgical management of UPJ obstruction is aimed at providing symptomatic relief and preserving any remaining renal function. Management choices include antegrade or retrograde endopyelotomy and open or laparoscopic pyeloplasty (77). Traditionally, open pyeloplasty has been the favored surgical treatment for UPJ obstruction; now, however, it is being replaced by minimally invasive procedures such as endopyelotomy and laparoscopic dismembered pyeloplasty (transperitoneal or retroperitoneal), which have a lower morbidity and cost (77). Endopyelotomy may be performed in the absence of crossing vessels. Given the hemorrhagic complications and the higher failure and recurrence rates of endopyelotomy if crossing vessels are present (70), laparoscopic dismembered pyeloplasty is currently considered to be the treatment of choice (77).

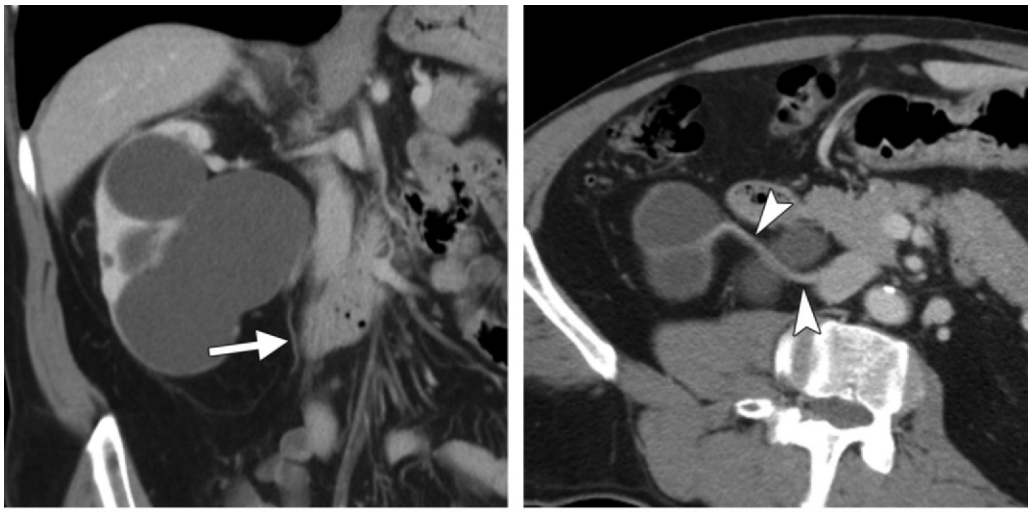

a. b.

Figure 21. UPJ obstruction in a 55-year-old man with a 2-year history of worsening postprandial abdominal pain. The patient had normal findings at urinalysis and no flank pain. **(a)** Coronal reformatted image from an abdominal CT study shows severe right-sided hydronephrosis with cortical thinning and a decompressed proximal ureter (arrow). **(b)** Axial CT image shows an accessory right renal vein (arrowheads) draining into the IVC and crossing the UPJ. The accessory vein was believed to be the cause of the UPJ obstruction in this case.

Vascular Compression of the Ureter

Pathogenesis and Clinical Presentation

Compression of the ureter may rarely occur if the ureter takes a retrovascular (retroiliac or retrocaval) course (78,79). Compression can also occur at the point of intersection of the ureter with retroperitoneal vascular structures. The implicated vessel is generally a dilated or aberrant ovarian vein (resulting in OVS); very rarely, the testicular vein is implicated (80–82). Since first being described by Clarke in 1964, OVS has been described in several subsequent published reports (83,84). The ovarian vein crosses the ureter obliquely in the retroperitoneum at the L3 level and normally does not cause ureteral compression. The term *ovarian vein syndrome* refers to obstructive uropathy, which is right sided in about 95% of cases and is thought to be due to ureteral compression at the pelvic brim by a dilated, aberrant, or thrombosed ovarian vein. OVS is uncommon in nulliparous women and generally occurs during or after pregnancy. Whether the syndrome represents a true pathophysiologic entity remains controversial (80). Although observed infrequently, the instances of "extrinsic vascular indentation" of the ureter that we have most often encountered in our practice occur at the point where the distal ureter crosses over the iliac vessels at the pelvic brim. We have further noted this finding to be more common on the right side. In the cases we encountered, this ureteral indentation was causing only a mild or low-grade proximal hydroureter and hydronephrosis (Fig 22), the clinical significance of which remains uncertain.

Obstruction from ureteral compression can be mild with minimal or no symptoms, or it can be severe, resulting in flank pain, hematuria, or pyelonephritis (78,80).

Radiologic Findings

Prior to the advent of CT urography, the diagnosis of OVS was made with either IVU or retrograde urography. Cases of OVS show indirect findings of an oblique extrinsic impression on the ureter, with proximal hydroureter and a normal pelvic ureter (Fig 23) (80,85). In cases of a retrocaval ureter, there is medial deviation of the obstructed segment, resulting in a characteristic reverse J configuration with proximal hydroureter and hydronephrosis (78). CT urography performed in the nephropyelographic phase with a split-bolus contrast-enhanced technique is now the imaging method of choice, since it allows concurrent evaluation of the cause of compression, the implicated vessel, and the proximal dilatation. Findings are best depicted on coronal MPR images. Three-dimensional VR can yield IVU-like images. Other causes of ureteral compression (both intrinsic and extrinsic) are easily excluded with CT urography.

Treatment

Treatment is not needed for low-grade obstruction or in asymptomatic cases. Surgical intervention to relieve the obstruction is indicated in symptomatic cases or if moderate or severe

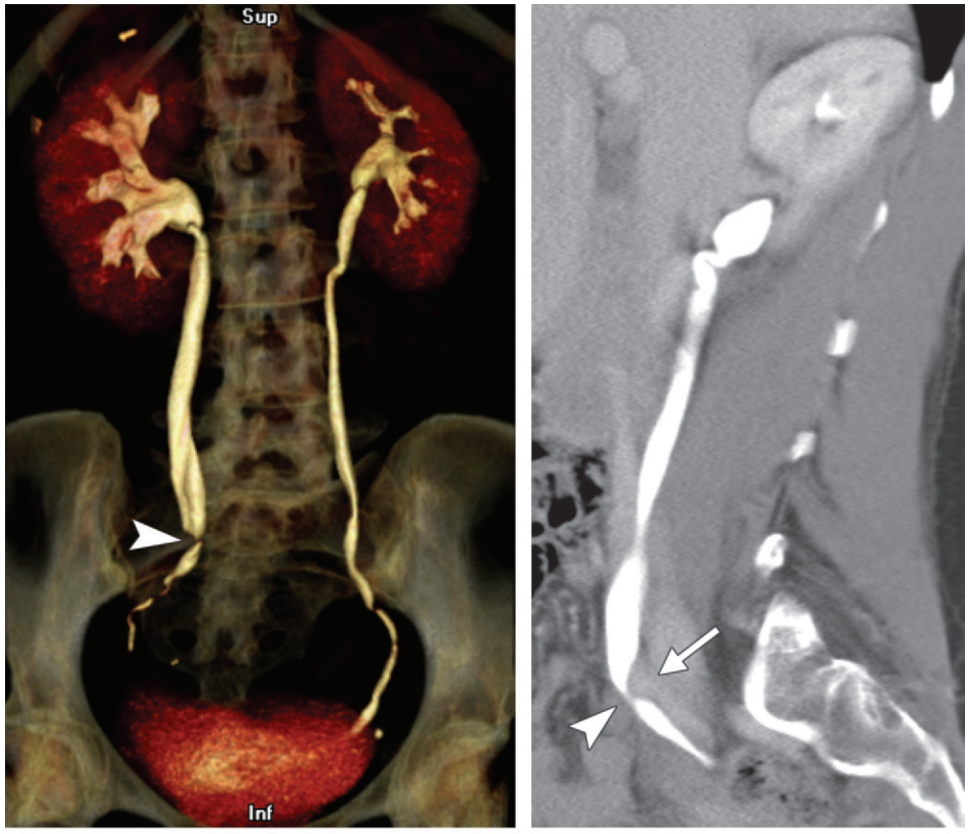

a. b.

Figure 22. Distal ureteral compression in a 39-year-old woman with hematuria. Three-dimensional VR **(a)** and sagittal reformatted **(b)** images from a CT urographic study show a mild extrinsic indentation (arrowhead) on the distal right ureter resulting from its crossing over the right CIA (arrow in **b**), causing mild proximal hydroureter and hydronephrosis.

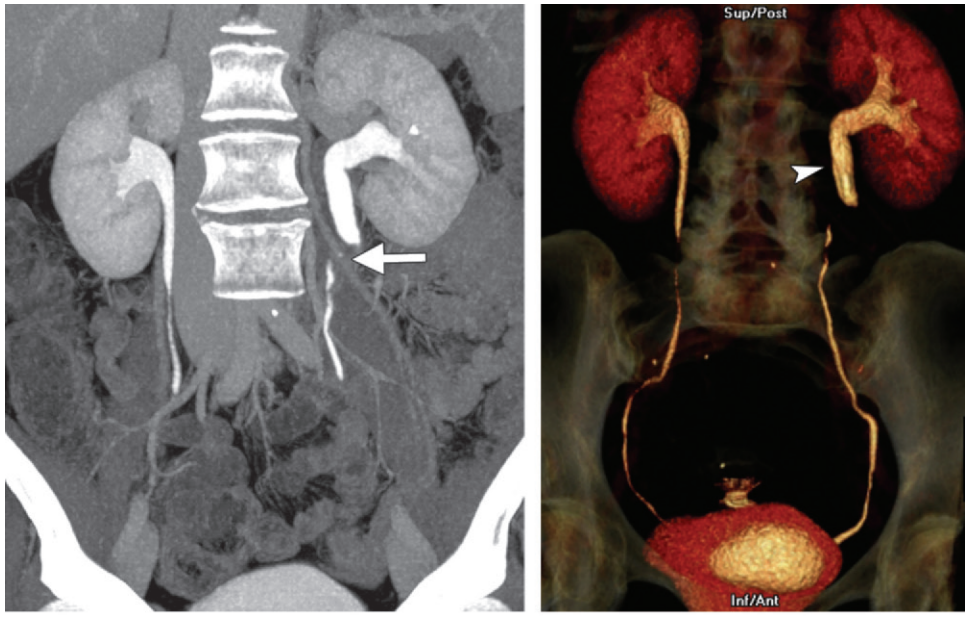

a. b.

Figure 23. Proximal ureteral compression in a 57-year-old woman with left-sided abdominal pain, a sensation of flank fullness, and hematuria. Coronal reformatted **(a)** and 3D VR **(b)** images from a CT urographic study show mild proximal left hydroureter (arrowhead in **b**) and hydronephrosis, findings that are the result of extrinsic compression by a crossing left ovarian vein (arrow in **a**).

hydronephrosis is present. Laparoscopic ureteroureterostomy, which involves transection and relocation of the ureter anterior to the IVC with subsequent reanastomosis, is the preferred surgical procedure for retrocaval ureters (86). Transcatheter ovarian vein embolization and surgical ligation (which is now performed laparoscopically) have been used to treat OVS (80).

Conclusion

Vascular structures in the abdomen and pelvis can compress or be compressed by adjacent anatomic structures. Such compression may be asymptomatic or may result in clinical syndromes that manifest with nonspecific and obscure symptoms, causing delayed or erroneous diagnoses. Multidetector CT, with isotropic data sets allowing reconstruction in the plane of these anatomic structures, provides a novel imaging perspective on these syndromes. Controversy remains as to the true anatomic mechanisms that cause such compressions, their relationship with symptoms, and the treatment of these syndromes.

Acknowledgments.—The authors thank Desiree Lazo for her administrative assistance; Christopher M. Brown for the illustrations; Julie Ostoich for editing the images; and William C. Pevec, MD, Tamas Vidovszky, MD, and Robert A. Jesinger, MD, for contributing images.

References

1. Harjola PT. A rare obstruction of the coeliac artery: report of a case. Ann Chir Gynaecol Fenn 1963;52:547–550.
2. Skandalakis JEGS, Rowe JS Jr. Surgical anatomy of the diaphragm. In: Nyhus LMBR, ed. Mastery of surgery. Boston, Mass: Little, Brown, 1984.
3. Curl JH, Thompson NW, Stanley JC. Median arcuate ligament compression of the celiac and superior mesenteric arteries. Ann Surg 1971;173(2): 314–320.
4. Horton KM, Talamini MA, Fishman EK. Median arcuate ligament syndrome: evaluation with CT angiography. RadioGraphics 2005;25(5):1177–1182.
5. Soman S, Sudhakar SV, Keshava SN. Celiac axis compression by median arcuate ligament on computed tomography among asymptomatic persons. Indian J Gastroenterol 2010;29(3):121–123.
6. Lee VS, Morgan JN, Tan AG, et al. Celiac artery compression by the median arcuate ligament: a pitfall of end-expiratory MR imaging. Radiology 2003;228(2):437–442.
7. Johnston KW, Lindsay TF, Walker PM, Kalman PG. Mesenteric arterial bypass grafts: early and late results and suggested surgical approach for chronic and acute mesenteric ischemia. Surgery 1995;118(1):1–7.
8. Mensink PB, van Petersen AS, Geelkerken RH, Otte JA, Huisman AB, Kolkman JJ. Clinical significance of splanchnic artery stenosis. Br J Surg 2006; 93(11):1377–1382.
9. Suzuki K, Tachi Y, Ito S, et al. Endovascular management of ruptured pancreaticoduodenal artery aneurysms associated with celiac axis stenosis. Cardiovasc Intervent Radiol 2008;31(6):1082–1087.
10. Erden A, Yurdakul M, Cumhur T. Marked increase in flow velocities during deep expiration: a duplex Doppler sign of celiac artery compression syndrome. Cardiovasc Intervent Radiol 1999;22 (4):331–332.
11. Reilly LM, Ammar AD, Stoney RJ, Ehrenfeld WK. Late results following operative repair for celiac artery compression syndrome. J Vasc Surg 1985;2 (1):79–91.
12. Takach TJ, Livesay JJ, Reul GJ Jr, Cooley DA. Celiac compression syndrome: tailored therapy based on intraoperative findings. J Am Coll Surg 1996; 183(6):606–610.
13. van Petersen AS, Vriens BH, Huisman AB, Kolkman JJ, Geelkerken RH. Retroperitoneal endoscopic release in the management of celiac artery compression syndrome. J Vasc Surg 2009;50(1): 140–147.
14. Roseborough GS. Laparoscopic management of celiac artery compression syndrome. J Vasc Surg 2009;50(1):124–133.
15. Gloviczki P, Duncan AA. Treatment of celiac artery compression syndrome: does it really exist? Perspect Vasc Surg Endovasc Ther 2007;19(3): 259–263.
16. von Rokitansky C. Lehrburch der pathologischen anatomie. Vienna, Austria: Braumuller & Seidel, 1861.
17. Wilkie DPD. Chronic duodenal ileus. Am J Med Sci 1927;173(5):643–648.
18. Agrawal GA, Johnson PT, Fishman EK. Multidetector row CT of superior mesenteric artery syndrome. J Clin Gastroenterol 2007;41(1):62–65.
19. Konen E, Amitai M, Apter S, et al. CT angiography of superior mesenteric artery syndrome. AJR Am J Roentgenol 1998;171(5):1279–1281.
20. Gustafsson L, Falk A, Lukes PJ, Gamklou R. Diagnosis and treatment of superior mesenteric artery syndrome. Br J Surg 1984;71(7):499–501.
21. Mansberger AR Jr, Hearn JB, Byers RM, Fleisig N, Buxton RW. Vascular compression of the duodenum: emphasis on accurate diagnosis. Am J Surg 1968;115(1):89–96.
22. Merrett ND, Wilson RB, Cosman P, Biankin AV. Superior mesenteric artery syndrome: diagnosis and treatment strategies. J Gastrointest Surg 2009;13(2):287–292.
23. Welsch T, Büchler MW, Kienle P. Recalling superior mesenteric artery syndrome. Dig Surg 2007; 24(3):149–156.
24. Sapkas G, O'Brien JP. Vascular compression of the duodenum (cast syndrome) associated with the treatment of spinal deformities: a report of six cases. Arch Orthop Trauma Surg 1981;98(1):7–11.
25. Griffiths GJ, Whitehouse GH. Radiological features of vascular compression of the duodenum occurring as a complication of the treatment of scoliosis (the cast syndrome). Clin Radiol 1978;29(1):77–83.
26. Hughes JP, McEntire JE, Setze TK. Cast syndrome: duodenal dilation or obstruction in a patient in a body cast, with review of the literature. Arch Surg 1974;108(2):230–232.
27. Strong EK. Mechanics of arteriomesenteric duodenal obstruction and direct surgical attack upon etiology. Ann Surg 1958;148(5):725–730.
28. Tsirikos AI, Jeans LA. Superior mesenteric artery syndrome in children and adolescents with spine

deformities undergoing corrective surgery. J Spinal Disord Tech 2005;18(3):263–271.
29. Hines JR, Gore RM, Ballantyne GH. Superior mesenteric artery syndrome: diagnostic criteria and therapeutic approaches. Am J Surg 1984;148 (5):630–632.
30. Applegate GR, Cohen AJ. Dynamic CT in superior mesenteric artery syndrome. J Comput Assist Tomogr 1988;12(6):976–980.
31. Unal B, Aktaş A, Kemal G, et al. Superior mesenteric artery syndrome: CT and ultrasonography findings. Diagn Interv Radiol 2005;11(2):90–95.
32. Lippl F, Hannig C, Weiss W, Allescher HD, Classen M, Kurjak M. Superior mesenteric artery syndrome: diagnosis and treatment from the gastroenterologist's view. J Gastroenterol 2002;37(8):640–643.
33. Wyten R, Kelty CJ, Falk GL. Laparoscopic duodenojejunostomy for the treatment of superior mesenteric artery (SMA) syndrome: case series. J Laparoendosc Adv Surg Tech A 2010;20(2):173–176.
34. Taheri SA, Williams J, Powell S, et al. Iliocaval compression syndrome. Am J Surg 1987;154(2): 169–172.
35. Cockett FB, Thomas ML. The iliac compression syndrome. Br J Surg 1965;52(10):816–821.
36. May R, Thurner J. The cause of the predominantly sinistral occurrence of thrombosis of the pelvic veins. Angiology 1957;8(5):419–427.
37. Thijs W, Rabe KF, Rosendaal FR, Middeldorp S. Predominance of left-sided deep vein thrombosis and body weight. J Thromb Haemost 2010;8(9): 2083–2084.
38. Mickley V, Schwagierek R, Rilinger N, Görich J, Sunder-Plassmann L. Left iliac venous thrombosis caused by venous spur: treatment with thrombectomy and stent implantation. J Vasc Surg 1998;28 (3):492–497.
39. Moudgill N, Hager E, Gonsalves C, Larson R, Lombardi J, DiMuzio P. May-Thurner syndrome: case report and review of the literature involving modern endovascular therapy. Vascular 2009;17(6): 330–335.
40. Oguzkurt L, Tercan F, Pourbagher MA, Kizilkilic O, Turkoz R, Boyvat F. Computed tomography findings in 10 cases of iliac vein compression (May-Thurner) syndrome. Eur J Radiol 2005;55 (3):421–425.
41. Chung JW, Yoon CJ, Jung SI, et al. Acute iliofemoral deep vein thrombosis: evaluation of underlying anatomic abnormalities by spiral CT venography. J Vasc Interv Radiol 2004;15(3):249–256.
42. Wolpert LM, Rahmani O, Stein B, Gallagher JJ, Drezner AD. Magnetic resonance venography in the diagnosis and management of May-Thurner syndrome. Vasc Endovascular Surg 2002;36(1): 51–57.
43. Elsharawy M, Elzayat E. Early results of thrombolysis vs anticoagulation in iliofemoral venous thrombosis: a randomised clinical trial. Eur J Vasc Endovasc Surg 2002;24(3):209–214.
44. Patel NH, Stookey KR, Ketcham DB, Cragg AH. Endovascular management of acute extensive iliofemoral deep venous thrombosis caused by May-Thurner syndrome. J Vasc Interv Radiol 2000;11 (10):1297–1302.
45. Heniford BT, Senler SO, Olsofka JM, Carrillo EH, Bergamini TM. May-Thurner syndrome: management by endovascular surgical techniques. Ann Vasc Surg 1998;12(5):482–486.
46. Alimi YS, DiMauro P, Fabre D, Juhan C. Iliac vein reconstructions to treat acute and chronic venous occlusive disease. J Vasc Surg 1997;25(4):673–681.
47. Grant JCB. A method of anatomy: descriptive and deductive. 3rd ed. Baltimore, Md: Williams & Wilkins, 1944.
48. El-Sadr AR, Mina E. Anatomical and surgical aspects in the operative management of varicocele. Urol Cutaneous Rev 1950;54(5):257–262.
49. de Schepper A. "Nutcracker" phenomenon of the renal vein and venous pathology of the left kidney [in Dutch]. J Belge Radiol 1972;55(5):507–511.
50. Menard MT. Nutcracker syndrome: when should it be treated and how? Perspect Vasc Surg Endovasc Ther 2009;21(2):117–124.
51. Kurklinsky AK, Rooke TW. Nutcracker phenomenon and nutcracker syndrome. Mayo Clin Proc 2010;85(6):552–559.
52. Fu WJ, Hong BF, Xiao YY, et al. Diagnosis of the nutcracker phenomenon by multislice helical computed tomography angiography. Chin Med J (Engl) 2004;117(12):1873–1875.
53. Arima M, Hosokawa S, Ogino T, Ihara H, Terakawa T, Ikoma F. Ultrasonographically demonstrated nutcracker phenomenon: alternative to angiography. Int Urol Nephrol 1990;22(1):3–6.
54. Scultetus AH, Villavicencio JL, Gillespie DL. The nutcracker syndrome: its role in the pelvic venous disorders. J Vasc Surg 2001;34(5):812–819.
55. Rudloff U, Holmes RJ, Prem JT, Faust GR, Moldwin R, Siegel D. Mesoaortic compression of the left renal vein (nutcracker syndrome): case reports and review of the literature. Ann Vasc Surg 2006;20(1):120–129.
56. Kim SH, Cho SW, Kim HD, Chung JW, Park JH, Han MC. Nutcracker syndrome: diagnosis with Doppler US. Radiology 1996;198(1):93–97.
57. Park SJ, Lim JW, Cho BS, Yoon TY, Oh JH. Nutcracker syndrome in children with orthostatic proteinuria: diagnosis on the basis of Doppler sonography. J Ultrasound Med 2002;21(1):39–45.
58. Cheon JE, Kim WS, Kim IO, et al. Nutcracker syndrome in children with gross haematuria: Doppler sonographic evaluation of the left renal vein. Pediatr Radiol 2006;36(7):682–686.
59. Beinart C, Sniderman KW, Tamura S, Vaughan ED Jr, Sos TA. Left renal vein to inferior vena cava pressure relationship in humans. J Urol 1982;127 (6):1070–1071.
60. Reed NR, Kalra M, Bower TC, Vrtiska TJ, Ricotta JJ 2nd, Gloviczki P. Left renal vein transposition for nutcracker syndrome. J Vasc Surg 2009;49(2):386–393; discussion 393–394.
61. Tripp BM, Homsy YL. Neonatal hydronephrosis: the controversy and the management. Pediatr Nephrol 1995;9(4):503–509.
62. Park JM, Bloom DA. The pathophysiology of UPJ obstruction: current concepts. Urol Clin North Am 1998;25(2):161–169.
63. Mayo WJ, Braasch WF, MacCarty WC. Relation of anomalous renal blood vessels to hydronephrosis. J Am Med Assoc 1909;LII(18):1383–1388.
64. Stephens FD. Ureterovascular hydronephrosis and the "aberrant" renal vessels. J Urol 1982;128(5): 984–987.
65. Gupta M, Smith AD. Crossing vessels: endourologic implications. Urol Clin North Am 1998;25 (2):289–293.
66. Frauscher F, Janetschek G, Helweg G, Strasser H, Bartsch G, zur Nedden D. Crossing vessels at the

ureteropelvic junction: detection with contrast-enhanced color Doppler imaging. Radiology 1999; 210(3):727–731.
67. Zeltser IS, Liu JB, Bagley DH. The incidence of crossing vessels in patients with normal ureteropelvic junction examined with endoluminal ultrasound. J Urol 2004;172(6 pt 1):2304–2307.
68. Richstone L, Seideman CA, Reggio E, et al. Pathologic findings in patients with ureteropelvic junction obstruction and crossing vessels. Urology 2009;73(4):716–719; discussion 719.
69. Sampaio FJ, Favorito LA. Ureteropelvic junction stenosis: vascular anatomical background for endopyelotomy. J Urol 1993;150(6):1787–1791.
70. Van Cangh PJ, Wilmart JF, Opsomer RJ, Abi-Aad A, Wese FX, Lorge F. Long-term results and late recurrence after endoureteropyelotomy: a critical analysis of prognostic factors. J Urol 1994;151 (4):934–937.
71. Veyrac C, Baud C, Lopez C, Couture A, Saguintaah M, Averous M. The value of colour Doppler ultrasonography for identification of crossing vessels in children with pelvi-ureteric junction obstruction. Pediatr Radiol 2003;33(11):745–751.
72. Keeley FX Jr, Moussa SA, Miller J, Tolley DA. A prospective study of endoluminal ultrasound versus computerized tomography angiography for detecting crossing vessels at the ureteropelvic junction. J Urol 1999;162(6):1938–1941.
73. Hendrikx AJ, Nadorp S, De Beer NA, Van Beekum JB, Gravas S. The use of endoluminal ultrasonography for preventing significant bleeding during endopyelotomy: evaluation of helical computed tomography vs endoluminal ultrasonography for detecting crossing vessels. BJU Int 2006;97(4):786–789.
74. Calder AD, Hiorns MP, Abhyankar A, Mushtaq I, Olsen OE. Contrast-enhanced magnetic resonance angiography for the detection of crossing renal vessels in children with symptomatic ureteropelvic junction obstruction: comparison with operative findings. Pediatr Radiol 2007;37(4):356–361.
75. Khaira HS, Platt JF, Cohan RH, Wolf JS, Faerber GJ. Helical computed tomography for identification of crossing vessels in ureteropelvic junction obstruction: comparison with operative findings. Urology 2003;62(1):35–39.
76. Braun P, Guilabert JP, Kazmi F. Multidetector computed tomography arteriography in the preoperative assessment of patients with ureteropelvic junction obstruction. Eur J Radiol 2007;61(1):170–175.
77. Wolf JS. Laparoscopic transperitoneal pyeloplasty. J Endourol 2011;25(2):173–178.
78. Brito RR, Zulian R, Albuquerque J, Borges HJ. Retrocaval ureter. Br J Urol 1973;45(2):144–152.
79. Nguyen DH, Koleilat N, Gonzalez R. Retroiliac ureter in a male newborn with multiple genitourinary anomalies: case report and review of the literature. J Urol 1989;141(6):1400–1403.
80. Bhutta HY, Walsh SR, Tang TY, Walsh CA, Clarke JM. Ovarian vein syndrome: a review. Int J Surg 2009;7(6):516–520.
81. Derrick FC Jr, Rosenblum R, Frensilli FJ. Right ovarian vein syndrome: six-year critique. Urology 1973;1(5):383–385.
82. Meyer JI, Wilbur AC, Lichtenberg R. Ureteric obstruction by the right testicular vein: CT diagnosis. Urol Radiol 1992;13(4):233–236.
83. Clark J. The right ovarian vein syndrome. In: Emmet J, ed. Clinical urography: an atlas and textbook of roentgenologic diagnosis. 2nd ed. Philadelphia, Pa: Saunders, 1964; 1227.
84. Tourné G, Ducroux A, Bourbon M, Blinding H. The ovarian vein syndrome: eight cases and review of the literature [in French]. J Gynecol Obstet Biol Reprod (Paris) 2002;31(5):471–477.
85. Shah MS, Tozzo PJ. Right ovarian vein syndrome. Urology 1974;3(4):488–490.
86. Li HZ, Ma X, Qi L, Shi TP, Wang BJ, Zhang X. Retroperitoneal laparoscopic ureteroureterostomy for retrocaval ureter: report of 10 cases and literature review. Urology 2010;76(4):873–876.

Multidetector CT of Vascular Compression Syndromes in the Abdomen and Pelvis

Ramit Lamba, MBBS, MD • Dawn T. Tanner, MD • Simran Sekhon, MBBS • John P. McGahan, MD • Michael T. Corwin, MD • Chandana G. Lall, MD

RadioGraphics 2014; 34:93–115 • **Published online** 10.1148/rg.341125010 • **Content Codes:** CT GI IR VA

Page 93
Thus, compression of the proximal celiac artery, transverse duodenum, left common iliac vein (CIV), left renal vein (LRV), ureteropelvic junction (UPJ), and ureter can occur due to their close anatomic relationship to adjacent ligaments as well as bony and vascular structures.

Page 93
Anatomic or morphologic findings that predispose to such compression may occasionally be encountered in asymptomatic patients who undergo imaging for unrelated causes. Thus, caution should be exercised to avoid overdiagnosis of these syndromes. It is important that the diagnosis of these syndromes not be based on imaging findings alone.

Page 96
Thus, isolated celiac compression during expiration may not be clinically significant. Severe compression occurs in only a small percentage of patients and may cause symptoms.

Page 104
Thus, anterior nutcracker syndrome may occur simultaneously with SMA syndrome. An association with a thin or asthenic body habitus has long been noted. Conceivably, all conditions that result in rapid weight loss and loss of retroperitoneal fat can predispose to nutcracker syndrome. It stands to reason that an AMA and AMD that can result in SMA syndrome would be enough to cause LRV compression as well.

Page 108
A crossing vessel can be a renal artery or renal vein (or both) that crosses the ureteric transition point—most commonly, an anteriorly crossing artery. The lower pole segmental artery and vein in particular have been implicated in UPJ obstruction.

RadioGraphics
Errata
May-June 2015 • Volume 35 • Number 3

Originally published in:

RadioGraphics 2014;34(1):93–115 • DOI: 10.1148/rg.341125010
Multidetector CT of Vascular Compression Syndromes in the Abdomen and Pelvis
Ramit Lamba, Dawn T. Tanner, Simran Sekhon, John P. McGahan, Michael T. Corwin, Chandana G. Lall

Erratum in:

RadioGraphics 2015;35(3):973 • DOI: 10.1148/rg.2015154007

Page 105, paragraph 2, lines 2–10: The sentences should read as follows: "A significantly higher ratio of **peak velocity** [not peak systolic velocity] at the point of renal vein compression to **peak velocity** [not peak systolic velocity] in the hilar renal vein has been reported in patients with nutcracker syndrome compared with asymptomatic control subjects (56,57). A **peak velocity** [not peak systolic velocity] ratio of over 4.7 has been reported to have a sensitivity of 100% and a specificity of 90% for the diagnosis (58)."

Page 109, Figure 18 legend, lines 4–5: The sentence should read as follows: "Duplex US showed a marked increase in **peak velocity** [not peak systolic velocity] distal to the narrowing."

Originally published in:

RadioGraphics 2015;35(2):387–399 • DOI: 10.1148/rg.352140095
Polypoid Lesions of the Gallbladder: Disease Spectrum with Pathologic Correlation
Vincent M. Mellnick, Christine O. Menias, Kumar Sandrasegaran, Amy K. Hara, Ania Z. Kielar, Elizabeth M. Brunt, Maria B. Majella Doyle, Nirvikar Dahiya, Khaled M. Elsayes

Erratum in:

RadioGraphics 2015;35(3):973 • DOI: 10.1148/rg.2015154008

Page 393, Figure 6c and 6d: The arrowheads on these images were incorrectly placed. The images are reprinted here with correctly placed arrows.

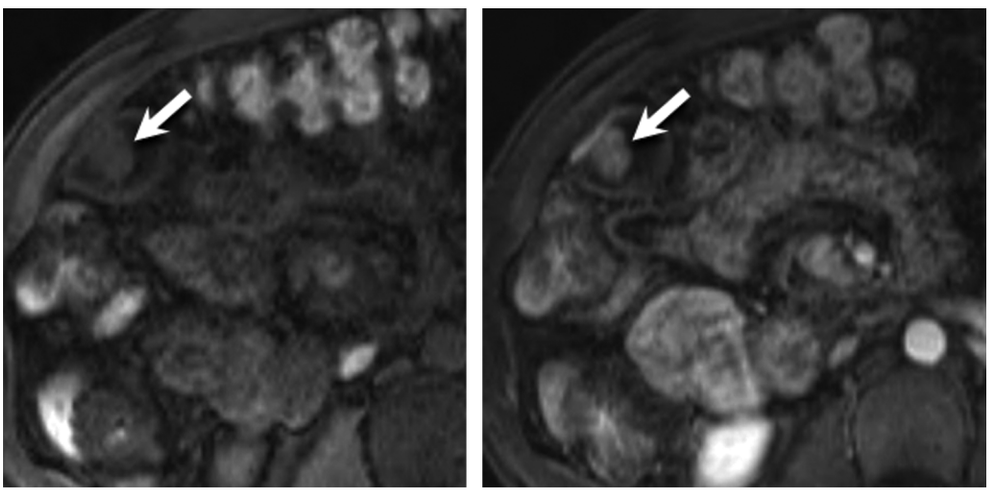

c. **d.**